Fall 2007

A nonlinear optimization approach for UPFC power flow control and voltage security

Radha P. Kalyani

Department: Electrical and Computer Engineering

A NONLINEAR OPTIMIZATION APPROACH FOR UPFC POWER FLOW CONTROL AND VOLTAGE SECURITY

by

RADHA PADMA KALYANI

A DISSERTATION

Presented to the Faculty of the Graduate School of the

UNIVERSITY OF MISSOURI-ROLLA

In Partial Fulfillment of the Requirements for the Degree

DOCTOR OF PHILOSOPHY

in

ELECTRICAL ENGINEERING

2007

_____	_____
Mariesa L. Crow, Co-Advisor	Daniel R. Tauritz, Co-Advisor
_____	_____
Jagannathan Sarangapani	Badrul H. Chowdhury

_____

Bruce M. McMillin

PUBLICATION DISSERTATION OPTION

This dissertation consists of publications which provide a Nonlinear Optimization method for determining the Long Term Control Settings of UPFC in steady state. The list of publications is as follows:

Paper 1 is "A Nonlinear Optimization Approach for UPFC Power Flow Control and Voltage Security: Sufficient System Constraints for optimality" (4 – 24) will be submitted for peer-revision under *IEEE Transactions on Power Systems*.

Paper 2 is "A Nonlinear Optimization Approach for UPFC Power Flow Control and Voltage Security" (25 – 45) will be submitted for peer-revision under *IEEE Transactions on Power Systems*.

Paper 3 is "Optimal Placement and Control of Unified Power Flow Control devices using Evolutionary Computing and Sequential Quadratic Programming" (46 – 60) was peer-reviewed and published in *Proceedings of the 2006 Power Systems Conference and Exposition*.

ABSTRACT

This dissertation provides a nonlinear optimization algorithm for the long term control of Unified Power Flow Controller (UPFC) to remove overloads and voltage violations by optimized control of power flows and voltages in the power network. It provides a control strategy for finding the long term control settings of one or more UPFCs by considering all the possible settings and all the (N-1) topologies of a power network. Also, a simple evolutionary algorithm (EA) has been proposed for the placement of more than one UPFC in large power systems.

In this publication dissertation, Paper 1 proposes the algorithm and provides the mathematical and empirical evidence. Paper 2 focuses on comparing the proposed algorithm with Linear Programming (LP) based corrective method proposed in literature recently and mitigating cascading failures in larger power systems. EA for placement along with preliminary results of the nonlinear optimization is given in Paper 3.

ACKNOWLEDGMENTS

I am grateful and indebted to my Ph.D. advisor Dr. Mariesa Crow who has given me another chance to prove myself and regain self-confidence. Her constant encouragement, support and sound advice at the time of need have been crucial factors for my successful completion of Ph.D. I love the way she gives one freedom to think and implement on their own which really inspires anyone to perform the best. It has been a great experience to work under her guidance through my PhD and a great opportunity to be a part of esteemed Power Group.

I thank Dr. Tauritz who has given a good start and trained me on various aspects of research. His constant feedback has helped me to find new heights in research. I thank Dr. Jag for showing a good path at crucial stage of my career and his feedback at time of need. I thank Dr. Chowdhury whose course work has been a stepping stone for success in research as well as for my internship. I thank Dr. McMillin for his invaluable feedback and support as a part of power group. Thanks to Sandia National Laboratories and UMR ECE department for the financial support through out my Ph.D.

I express my deep appreciation and gratitude to my parents and sister who have been with me through good and bad times. I am grateful to Regina Kohout and Frieda Adams for all their support and compassion. I thank all my friends who made my stay in Rolla pleasant and memorable.

Finally, I would like to dedicate this dissertation to my husband Shiva Sooryavaram without whom I would have not completed my Ph.D.

TABLE OF CONTENTS

Page

PUBLICATION DISSERTATION OPTION iii

ABSTRACT iv

ACKNOWLEDGMENTS v

LIST OF ILLUSTRATIONS ix

LIST OF TABLES xi

SECTION

1. INTRODUCTION 1

PAPER

1. A Nonlinear Optimization Approach for UPFC Power Flow Control and Voltage Security: Sufficient System Constraints for Optimality 4

Abstract 4

I. Introduction 4

II. The UPFC Power Injection Model 5

III. UPFC Objective Function 6

A. Power Flow Performance Index 6

B. Voltage Security Index 7

C. Cumulative Performance Index 7

IV. Nonlinear Optimization 9

A. Unconstrained Minimization [1], [2] 9

B. Constrained Minimization 9

V. Small Illustrative Example 11

A. Constrained Minimization of PI_{MVA} 11

B. Constrained Minimum of PI_V 14

C. Cumulative Analysis 15

VI. Sequential Quadratic Programming 16

VII. Simulation Results 16

A. Three bus system 16

B. 118 bus system 16

VIII. Conclusions 19

Acknowledgements 20
References 21
Appendix 23
2. A Nonlinear Optimization Approach for UPFC Power Flow Control and Voltage Security 25
Abstract 25
I. Introduction 25
II. The UPFC Power Injection Model 27
III.UPFC Objective Function 28
A. Power Flow Performance Index 28
B. Voltage Security Index 30
C. The Cumulative Performance Index 31
IV. Sequential Quadratic Programming 34
A. The SQP Algorithm 35
B. Quasi-Newton Approximation 36
C. Merit Function Sequential Quadratic Programming 36
V. Simulations Results 37
A. Line Outage 4-5 (IEEE 39 bus system) 37
B. Comparison of LP and SQP Nonlinear Optimization 37
1. Case I : UPFC on 16 - 17 38
2. Case II : UPFC on 15 - 16 39
3. Case III : UPFC on 4 - 14 39
C. Mitigating Cascading Failures in the IEEE 118 bus system 40
1. Scenerio I - line outage 4 - 5 41
2. Scenerio II - line outage 37 - 39 42
3. Scenerio III - line outage 89 - 92 42
VI. Conclusions 43
Acknowledgements 43
References 44
3. Optimal Placement and Control of Unified Power Flow Control Devices using Evolutionary Computing and Sequential Quadratic Programming 46
Abstract 46

I. Introduction 47
II. UPFC Placement and Control 48
III.UPFC Model 50
IV. UPFC Placement EA 51
A. Fitness Function 51
B. Representation 51
C. Initialization 52
D. Parent Selection & Recombination 52
E. Mutation 52
F. Reproduction Correction 54
G. Survivor Selection 54
H. Termination Condition 54
V. Simulations Results 55
VI. Conclusion 57
Acknowledgements 58
References 58
SECTION
2. SIMULATION RESULTS 61
2.1. RESULTS FOR *P* CONTROL 62
2.2. RESULTS FOR *Q* CONTROL 63
2.3. CONCLUSION 65
3. CONCLUSION 66
BIBLIOGRAPHY 67
VITA 68

LIST OF ILLUSTRATIONS

Figure Page

Paper 1

1. $Line_{ij}$ after UPFC installation 6

2. Three bus system after UPFC installation on line 2 - 3 12

3. Feasible region of δ_{34} and δ_{13} for positive definiteness of H_B 14

4. Control settings for a single placement 17

5. Line diagram of IEEE 118 bus power system 19

6. PQ control for single UPFC placement 19

Paper 2

1. Power injection model of UPFC 27

2. PI_{MVA} space for a single UPFC placement (13-14) and SLC (4-5) 29

3. PI_{MVA} space for two UPFC placements (13-14, 2-3) for SLC (4-5) 30

4. PI_V space for a single UPFC placement (13-14) and SLC (4-5) 32

5. PI_V curvature for two UPFC placements (13-14, 2-3) and SLC (4-5) 32

6. PI_{cum} curvature for a single UPFC placement (13-14) and SLC (4-5) 33

7. One line diagram of the IEEE 118 bus system 41

Paper 3

1. PI curvature for single UPFC placement 26-30 and SLC 23-32 49

2. PI surface for two UPFC placements 5-8, 26-30 and SLC 23-32 50

3. UPFC injection model 51

4. Example UPFC placement individual 52

5. UPFC initially placed on line 53-55 53

6. UPFC moved to the neighbouring line 53-54 as a result of mutation 53

7. Example invalid and valid placements 54

8. Comparison of EA and H for NOL 58

9. Comparison of EA and H for TOP 59

10. Comparison of EA and H for average PI 59

SECTION

2.1. Line diagram of IEEE 118 bus system 61

2.2. *P* control of the single UPFC placement 26-30 and SLC 23-32 62
2.3. *P* control for the two UPFC placements 5-8, 26-30 and SLC 23-32 63
2.4. *Q* control single UPFC placement 26-30 and SLC 23-32 64
2.5. *Q* control for the two UPFC placements 5-8, 26-30 and SLC 23-32 64

LIST OF TABLES

Table Page

Paper 1

I. Bus solution before UPFC installation for 3 bus system 17

II. Line Flow before UPFC installation for 3 bus system 18

III. Bus solution after UPFC installation for 3 bus system 18

IV. Line flow after UPFC installation for 3 bus system 18

V. Monte Carlo sampling test for 2 UPFCs 20

VI. Monte Carlo sampling test for 3 UPFCs with PQ control 20

Paper 2

I. Contigency analysis results without UPFC..... 38

II. Best placements for mitigating the overloads caused by 4-5 38

III. Comparison of SQP and LP powerflow control for placement 16-17 39

IV. Comparison of SQP and LP control parameters for placement 16-17..... 39

V. Comparison of SQP and LP powerflow control for placement 15-16 39

VI. Comparison of SQP and LP control parameters for placement 15-16..... 40

VII. Comparison of SQP and LP powerflow control for placement 4-14 40

VIII. Comparison of SQP and LP control parameters for placement 4-14 40

IX. SCENARIO 4-5 42

X. SCENARIO 37-39..... 42

XI. SCENARIO 89-92 43

Paper 3

I. Specifications of EA for placement of UPFC..... 51

II. EA Parameter sets..... 55

III. Mean and Standard Deviation of *HFit* over five runs..... 56

IV. Experimental results of WRST on three parameters sets..... 57

V. Comparison of ES, EA and H 57

SECTION

1. INTRODUCTION

Flexible AC Transmission systems (FACTS) are utilized to increase the capacity over existing transmission corridors by proper power flow control over designated routes and to provide voltage support in the network. The unified power flow controller (UPFC) is one such FACTS device which can simultaneously control the bus voltages and power flows on the transmission line in steady state. Given the fast acting corrective control, it is desirable to utilize the device to control power flows in order to relieve line overloads and transmission congestion as well as to provide voltage support.

The UPFC control system is functionally divided into long term control and dynamic control. The long term control defines the functional operating mode of the UPFC and is responsible for generating the dynamic control references for the series and shunt compensation to meet the prevailing demands of the transmission system. Thus an optimal control strategy is required for best performance of the device in real time under different operating modes.

The long term control algorithms described in the literature have been applied to a power system for a particular topology, load, and generation profile [1]-[5]. The described methods have been applied to static systems and did not consider the effect of all (N-1) outages in the network. A few researchers have considered the (N-1) topologies for placements [6]–[10] but not for determining the long term control settings (LTC) as it becomes computationally intensive. To date, only a few authors have developed algorithms for improving the transmission line loading profile over the entire set of

different topologies [11][12]. This dissertation proposes a nonlinear optimization algorithm for determining the optimal long term power flow control settings of one or more UPFCs over all possible topologies in the network. This dissertation also derives the system constraints under which the optimality is guaranteed. A comparison with recent corrective control techniques [12] shows the optimality of the settings. A simple GA is also used to find the near optimal placements in any given power network.

The mathematical formulation of the algorithm is given in Paper 1. The mathematical analysis of the objective function along with the power system constraints proved that the objective function search space is convex under certain system constraints. As the objective function is a convex nonlinear equation with nonlinear equality constraints, a nonlinear optimization method, the Sequential Quadratic Programming (SQP) method, is used to find the long term control settings. A thorough illustration of the derivation of the system constraints is provided for a small three bus system, and further generalized for the IEEE 118 bus power system. Monte Carlo trials are used to support the conjecture that the search space is convex for the large IEEE 118 bus system.

Paper 2 extends the application of the nonlinear SQP optimization algorithm proposed in Paper 1. It compares the SQP based long term control settings favorably with linear programming (LP) based optimal power flow (OPF) for the same constraints in the IEEE 39 bus system. This comparison shows that the placements and power flow control settings given by the SQP are preferable since the SQP results yield higher security margins for the power flows on the lines and voltages at the buses. Also further testing of the algorithm is conducted by finding placements and long term control settings that mitigate cascading failures in the IEEE 118 bus system.

Paper 3 shows the preliminary research conducted to find the best placement location and long term control settings of the UPFCs using Evolutionary Algorithms (EA) and an SQP based optimization method. It can be concluded from these results that the loadability of the system increased and better power flow control (during line outages) was achieved by choosing the optimal placement and control settings for the UPFCs. The results of the combination are compared with a greedy placement heuristic (H) [11] and the SQP based method. Comparison of the EA and SQP approach with the H and SQP approach showed that robust algorithms such as EAs can find the optimal/near optimal solution for the placement problem at minimum time expense.

PAPER 1

A Nonlinear Optimization Approach for UPFC Power Flow Control and Voltage Security: Sufficient System Constraints for Optimality

R. P. Kalyani, *Student Member, IEEE*, M. L. Crow, *Senior Member, IEEE*, and D. R. Tauritz, *Member, IEEE*

ABSTRACT

This paper derives the power system operating constraints under which the nonlinear sequential quadratic programming optimization algorithm is guaranteed to find the optimal long term control setting of one or more UPFCs. The algorithm is developed for a small 3 bus illustrative test system and then further applied on the IEEE 118 bus test power system.

***Index Terms*— FACTS, UPFC, Long Term Control, Performance Index, Sequential Quadratic Programming**

I. INTRODUCTION

The bulk power system forms one of the largest complex inter-connected networks ever built and its sheer size makes control and operation of the grid an extremely difficult task. Because the existing transmission system was not designed to meet the present demand, daily transmission constraints increase electricity costs to consumers and increase the risk of blackouts. Although transmission congestion could be greatly alleviated by adding new transmission lines, investment in new transmission facilities lags considerably behind investment in new generation and growth in electricity demand. Construction of high-voltage transmission

Kalyani and Crow are with the Electrical & Computer Engineering Department, University of Missouri-Rolla, Tauritz is with the Computer Science Department, University of Missouri-Rolla, Rolla, MO 65409-0810

facilities is expected to increase by only 6% during the next decade, whereas electricity demand and new generation capacity are each projected to increase by almost 20% [3]. The lag in transmission growth results from the difficulty in building new transmission lines due to public opposition that ranges from aesthetic to environmental reasons. Introducing advanced transmission technologies such as Flexible AC Transmission System (FACTS) devices could help reduce transmission congestion by providing precise and rapid control of power flow [4], [5]. FACTS devices are solid state converters that have the ability to control various electrical parameters in transmission networks. Unified Power Flow Controller (UPFC) is a FACTS device that can effectively control both the active and reactive flows on the lines and voltage magnitudes at the buses to which they are connected.

Most of the FACTS control setting algorithms described in the literature have been applied to a power system for a particular set topology, load, and generation profile [6]–[10]. The described methods were applied to static systems and did not consider the effect of topology changes due to line outages. To date, only a few authors have developed algorithms for improving the transmission line loading profile over the entire set of possible single line contingencies [11], [12]. The nonlinear Sequential Quadratic Programming (SQP) algorithm was first applied to the simultaneous powerflow control and voltage security problem in [13] and was shown to produce accurate results with computational efficiency. However, it was noted that an optimal solution is only guaranteed if the search space is convex. In this paper, the power system operating constraints will be derived such that the search space of SQP is convex, thus guaranteeing an optimal solution to the UPFC powerflow control and voltage security optimization.

II. The UPFC Power Injection Model

The UPFC is a device that is capable of controlling voltage magnitudes as well as the active and reactive power flows simultaneously. In this paper, the active and reactive powers on the adjacent transmission line are controlled to minimize overloading along transmission corridors and maintain voltage security across the set of all possible contingencies. Fig. 1 shows the power injection model of a lossless UPFC utilized in the algorithm development and simulation results [14]. To incorporate the UPFC into a powerflow program, the transmission line must

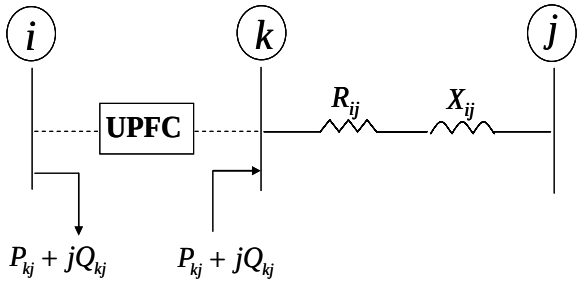

Fig. 1. $Line_{ij}$ after UPFC installation

be modified to accurately represent the UPFC characteristics. To install a UPFC at bus i on transmission line $i-j$, a fictitious bus k is introduced between buses *i* and *j*, as shown in Fig. 1. This model is consistent with the UPFC model for power flow control proposed in [14] where the sending end bus is modeled as a "PV" bus and the receiving end is modeled as a "PQ" bus. The UPFC device is assumed to be capable of altering the power flow through line $i-j$ by $\pm$ 20% of the original line capacity, S_{ij}^{max}.

III. UPFC Objective Function

To determine the optimal powerflow and voltage settings for the UPFC, it is necessary to define an objective function that measures the "goodness" of a particular setting. In this paper, the objective function is derived from the power flow constraints and the voltage security margin.

A. Power Flow Performance Index

The Power Flow Performance Index (PI_{MVA}) is used to assess the performance of all possible UPFC power flow settings over the set of all single line contingencies (SLCs). This performance index measures the aggregate amount of power that exceeds the line capacities. Minimizing PI_{MVA} effectively minimizes all line overloads since higher overloads incur heavier penalties than lower overloads. This produces better utilization of all lines in the system since, even when no lines are overloaded, minimizing PI_{MVA} may cause underloaded lines to be more heavily utilized. The power flow performance index is given by:

$$PI_{MVA} = \sum_{all\,lines} \left(\frac{S_{ij}}{S_{ij}^{max}}\right)^2 \tag{1}$$

S_{ij} apparent power flow on line $i-j$ for each SLC

S_{ij}^{max} maximum power flow on line $i-j$

B. Voltage Security Index

Voltage security is concerned with the ability of a power system to maintain acceptable voltages at all buses under normal conditions and after being subjected to a line outage. Excessive voltage changes can occur following a severe contingency. To avert this situation, several voltage performance indices have been proposed and utilized to find the critical bus which signifies voltage insecurity in the event of a line outage [15]–[21]. An analysis of these indices indicates that the Voltage Security Index (PI_V) [18], [22] captures the desired voltage security indicators and additionally is similar in construct to that of PI_{MVA}. The PI_V used in this paper is

$$PI_V = W_V \sum_{i=1}^{N} \left(\frac{V_i - V_i^{ss}}{\triangle V_i^{lim}} \right)^2 \tag{2}$$

where

V_i voltage magnitude at bus *i*

V_i^{ss} voltage magnitude at bus *i* in steady state

$\triangle V_i^{lim}$ voltage deviation limit, above which voltage deviations are unacceptable

N number of buses

W_V nonnegative weighting factor

C. Cumulative Performance Index

According to classical contingency screening techniques, two separate ranking lists are often required for power flow and voltage profile problems respectively, since the contingencies causing line overloads do not necessarily cause bus voltage violations and vice versa. Thus, the two performance indices, which give measures for line overloads (PI_{MVA}) and bus voltage violations (PI_V), respectively, are cumulatively utilized to form the objective function for determining the control settings in this paper. The Cumulative Performance Index (PI_{cum}) is:

$$\text{Min } PI_{cum} = \sum_{all\ lines} \left(\frac{S_{ij}}{S_{ij}^{max}} \right)^2 + W_V \sum_{i=1}^{N} \left(\frac{V_i - V_i^{ss}}{\triangle V_i^{lim}} \right)^2 \tag{3}$$

Subjected to

Equality Constraints:

$$0 = \triangle P_i - \sum_{j=1}^{N} V_i V_j Y_{ij} \cos(\theta_i - \theta_j - \phi_{ij})$$

$$0 = \triangle Q_i - \sum_{j=1}^{N} V_i V_j Y_{ij} \sin(\theta_i - \theta_j - \phi_{ij})$$

for $i=1,...,N$ and $j=1,...,N$

Inequality Constraints:

$$P_i^{min} \leq P_i \leq P_i^{max}$$

$$Q_i^{min} \leq Q_i \leq Q_i^{max}$$

$$V_i^{min} \leq V_i \leq V_i^{max}$$

UPFC Constraints:

$$\sqrt{P_{SET}^2 + Q_{SET}^2} \leq S_{ij}^{max}$$

P_i	Active power generation at bus *i*
Q_i	Reactive power generation at bus *i*
P_i^{min}	Minimum active power generation at bus *i*
P_i^{max}	Maximum active power generation at bus *i*
Q_i^{min}	Minimum reactive power generation at bus *i*
Q_i^{max}	Maximum reactive power generation at bus *i*
V_i	Voltage magnitude at bus *i*
V_i^{min},V_i^{max}	Min and max voltage magnitude at bus *i*
V_j	Voltage magnitude at bus *j*
Y_{ij}	Magnitude of the (i, j) element of the admittance matrix
ϕ_{ij}	Angle of the (i, j) element of the admittance matrix
P_{SET}, Q_{SET}	Active and reactive UPFC control settings

IV. Nonlinear Optimization

To guarantee that SQP nonlinear optimization will converge to an optimal point, it is necessary to find the system conditions under which the search space is convex [1]. To establish the convexity of the search space, both unconstrained and constrained systems will be discussed.

A. Unconstrained Minimization [1], [2]

A continuous, twice differentiable function of several variables is convex if and only if its Hessian matrix *H($\bar{x}$)* is positive definite, where the Hessian matrix for the *n* variable function $f(x_1, x_2, ...x_n)$ is comprised of the second-order partial derivatives (4). Thus if *H($\bar{x}$)* is positive definite everywhere, then the objective function is guaranteed to have a global minimum.

$$H(\bar{x}) = \begin{bmatrix} \frac{\partial^2 f(\bar{x})}{\partial x_1^2} & \cdots & \frac{\partial^2 f(\bar{x})}{\partial x_1 x_n} \\ & \vdots & \\ \frac{\partial^2 f(\bar{x})}{\partial x_n x_1} & \cdots & \frac{\partial^2 f(\bar{x})}{\partial x_n^2} \end{bmatrix} \tag{4}$$

B. Constrained Minimization

Most optimization problems, however, are constrained and require simultaneous minimization while meeting the system equality (and inequality) constraints. The usual method of solving a constrained minimization is to introduce Lagrangian multipliers to solve:

$$\text{Min } f\left(x_1, x_2, ..., x_n\right) \tag{5}$$

with equality constraints

$$g_1(x_1, ..., x_n) = 0$$

$$\vdots$$

$$g_m(x_1, ..., x_n) = 0$$

where $1 \leq m \leq n$. The constraints of the problem can be accommodated into the objective function by formulating the Lagrangian function:

$$L\left(x, \lambda\right) = f(x) - \lambda_1 g_1(x) - \lambda_2 g_2(x) \cdots - \lambda_m g_m(x) \tag{6}$$

According to optimization theory, the Karush-Kuhn-Tucker (KKT) necessary first order conditions of optimality are obtained by setting the first order derivatives of the Lagrangian function equal to zero [1], [2], [23]–[25]:

$$\begin{aligned} \frac{\partial}{\partial x_1} L(x^*, \lambda^*) &= 0 \\ &\vdots \\ \frac{\partial}{\partial x_n} L(x^*, \lambda^*) &= 0 \\ \frac{\partial}{\partial \lambda_1} L(x^*, \lambda^*) &= 0 \\ &\vdots \\ \frac{\partial}{\partial \lambda_n} L(x^*, \lambda^*) &= 0 \end{aligned} \tag{7}$$

where (x^*, λ^*) is the optimal solution of (5). For determining whether the solution (x^*, λ^*) obtained by solving (7) is an optimum, second order conditions must be utilized. This involves the formulation of H($\bar{x}$) with constraints on the border called a bordered Hessian (H_B) [24]. For an *n*-variable Lagrangian problem with *m* constraints, H_B is a *(n + m)* × *(n + m)* matrix:

$$H_B = \begin{bmatrix} H(\bar{x}) & J^T(x) \\ J(x) & 0 \end{bmatrix} \tag{8}$$

where *J(x)* has *m* rows and *n* columns, with the rows consisting of the first order derivatives of the constraint vectors (9) and H($\bar{x}$) is the Hessian based on the Lagrangian problem (10).

$$J(x) = \begin{bmatrix} \frac{\partial g_1}{\partial x_1} & \cdots & \frac{\partial g_1}{\partial x_n} \\ & \vdots & \\ \frac{\partial g_m}{\partial x_1} & \cdots & \frac{\partial g_m}{\partial x_n} \end{bmatrix} \tag{9}$$

$$H(\bar{x}) = \begin{bmatrix} \frac{\partial^2 L}{\partial x_1^2} & \cdots & \frac{\partial^2 L}{\partial x_1 x_n} \\ & \vdots & \\ \frac{\partial^2 L}{\partial x_n x_1} & \cdots & \frac{\partial^2 L}{\partial x_n^2} \end{bmatrix} \tag{10}$$

After constructing H_B as defined in (8), the *(n-m)* leading principal minors (LPM) starting from *(2m+1)* to *(n+m)* must be evaluated to determine the local minimum or maximum of the

constrained optimization. A positive definite H_B signifies the existence of a local minimum and a negative definite H_B signifies the existence of a local maximum for the constrained optimization problem. The matrix H_B is

1) positive definite if sign(LPM_{n+m}) = sign(det H_B) = $(-1)^m$ and the successive LPM's have the same sign
2) negative definite if (LPM_{n+m}) = sign(det H_B) = $(-1)^n$ and the successive LPM's from LPM_{2m+1} to LPM_{n+m} alternate in sign.

V. Small Illustrative Example

To guarantee that globally optimal power flow and voltage settings for the UPFC exist, the cumulative performance index must be convex. This implies that the H_B matrices of both the PI_{MVA} and PI_V indices should be positive definite. To analyze the constrained minimization of these objective functions, a simple 3 bus power system is chosen as an illustrative example [26]. In this system, the UPFC is installed on line 2–3 at bus 2 as shown Fig. 2. Bus 4 is the additional fictitious bus.

A. Constrained Minimization of PI_{MVA}

The theory of constrained minimization is applied to the PI_{MVA} of the 3 bus power system to find the conditions under which the constrained minimum is assured. For this system with *m* = 4 constraints and *n* = 6 variables, the Lagrangian is given by:

$$\begin{aligned} L &= \sum_{i \neq j} \left(\frac{V_i^4 Y_{ij}^2 + V_i^2 V_j^2 Y_{ij}^2 - 2V_i^3 V_j Y_{ij}^2 \cos(\delta_{ij})}{(S_{ij}^{max})^2} \right) \\ &\quad - \begin{bmatrix} \lambda_1 \\ \lambda_2 \\ \lambda_3 \\ \lambda_4 \end{bmatrix}^T \begin{bmatrix} \triangle P_2 \\ \triangle P_3 \\ \triangle Q_3 \\ \triangle P_4 \end{bmatrix} \end{aligned} \tag{11}$$

To minimize PI_{MVA}, the system variables that determine the convexity are the

1) angle differences across each line:
   - $\delta_{12} = \theta_1 - \theta_2$,
   - $\delta_{13} = \theta_1 - \theta_3$,

- $\delta_{24} = \theta_2 - \theta_4$,
- $\delta_{34} = \theta_3 - \theta_4$, and

2) voltage magnitudes V_3 and V_4.

The number of principal minors that must be assessed for determining the positive definiteness of this function are *(n-m)* = 2, one of dimension *(2m+1)* = 9 and another of dimension *(n+m)* = 10. Since the number of constraints in this case is four, the sign of the determinant should be positive, since $((-1)^4 > 0)$. The first principal minor (FPM) is a 9×9 matrix:

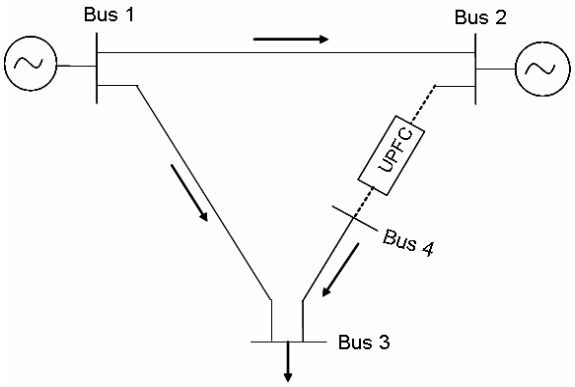

Fig. 2. Three bus system after UPFC installation on line 2 – 3

$$FPM = \left[\begin{array}{c|c} \begin{array}{c} Hessian \\ (5 \times 5) \end{array} & \begin{array}{c} Jacobian^T \\ (5 \times 4) \end{array} \\ \hline \begin{array}{c} Jacobian \\ (4 \times 5) \end{array} & \begin{array}{c} ZeroMatrix \\ (4 \times 4) \end{array} \end{array}\right] \tag{12}$$

The second principal minor (SPM) is the 10×10 bordered Hessian matrix given by:

$$H_B = SPM = \left[\begin{array}{c|c} \begin{array}{c} Hessian \\ (6 \times 6) \end{array} & \begin{array}{c} Jacobian^T \\ (6 \times 4) \end{array} \\ \hline \begin{array}{c} Jacobian \\ (4 \times 6) \end{array} & \begin{array}{c} ZeroMatrix \\ (4 \times 4) \end{array} \end{array}\right] \tag{13}$$

To ensure the positive definiteness of principal minors, the following relationships must hold:

$$11.50 \sin^2 (\delta_{12} - \phi_{12}) \quad > \quad 0 \tag{14}$$

$$1.09 \times 10^{-6} V_3^2 \, V_4^2 \sin^2(\delta_{12} - \phi_{12}) \sin^2 \delta_{24} \quad > \quad 0 \tag{15}$$

$$\begin{aligned} V_3^4 V_4^4 \sin^2(\delta_{12} - \phi_{12}) \sin^2 \delta_{24} \Big\{ & -1.80 \times 10^{-12} \sin^2(\delta_{13} - \phi_{13}) \\ & \sin^2(\delta_{34} - \phi_{34}) + 9.96 \times 10^{-5} \sin^2(\delta_{13} - \phi_{13}) \cos^2(\delta_{34} - \phi_{34}) \\ & +9.96 \times 10^{-5} \cos^2(\delta_{13} - \phi_{13}) \sin^2(\delta_{34} - \phi_{34}) + 1.15 \times 10^{-12} \\ & \cos^2(\delta_{13} - \phi_{13}) \cos^2(\delta_{34} - \phi_{34}) - 1.99 \times 10^{-3} \sin^2(\delta_{13} - \phi_{13}) \\ & \cos(\delta_{34} - \phi_{34}) \Big\} \quad > 0 \end{aligned} \tag{16}$$

$$(\text{Equation (A1) in the Appendix}) \tag{17}$$

It is obvious that constraints (14) and (15) will be satisfied for any angles, thus further discussion will focus on constraints (16) and (17).

Constraint (16) has both positive and negative leading coefficients, but noting that both the $\cos^2(\cdot)$ and $\sin^2(\cdot)$ terms are positive values between 0 and 1, it is clear that constraint (16) is dominated by the term:

$$-1.99 \times 10^{-3} \sin^2(\delta_{13} - \phi_{13}) \cos(\delta_{34} - \phi_{34}) \tag{18}$$

For this term to be positive requires that

$$\cos(\delta_{34} - \phi_{34}) < 0 \tag{19}$$

Following the same argument, constraint (17) requires that

$$\sin(\delta_{34} - \phi_{34}) \quad < \quad 0 \tag{20}$$

$$\cos(\delta_{13} - \phi_{13}) \quad < \quad 0 \tag{21}$$

$$\sin(\delta_{13} - \phi_{13}) \quad < \quad 0 \tag{22}$$

Fig. 3 shows the feasible regions of δ_{34} and δ_{13}. In summary, the conditions under which the 3 bus system achieves minimum of PI_{MVA} are such that the angle differences should be

- $-\pi < \delta_{12} < \pi$
- $-\pi + \phi_{13} < \delta_{13} < -\frac{\pi}{2} + \phi_{13}$
- $-\pi + \phi_{34} < \delta_{34} < -\frac{\pi}{2} + \phi_{34}$
- $-\frac{\pi}{2} < \delta_{24} < \frac{\pi}{2}$

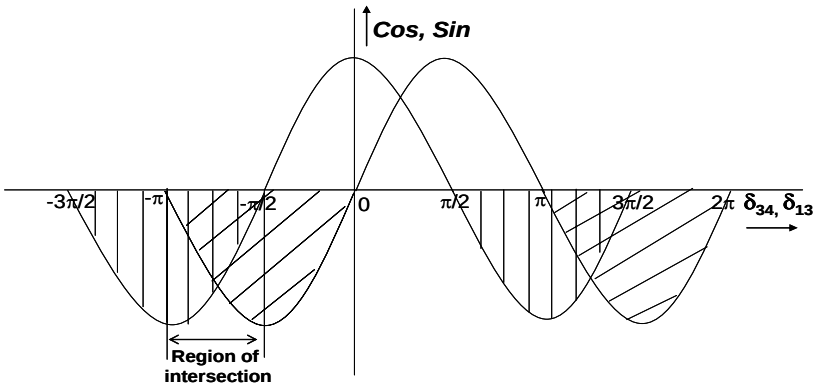

Fig. 3. Feasible region of δ_{34} and δ_{13} for positive definiteness of H_B

Further observance of the constraints (14) - (17) show that for any positive values of voltages V_3 and V_4 (11) will be positive definite. Thus considering steady operating conditions the voltages are assumed to be in the range [0.8, 1.2].

B. Constrained Minimum of PI_V

The active power injection of the UPFC is held constant to steady state active power flow while the reactive power is adjusted to find the minimum PI_V. Thus the change in active power flow at the bus, $\triangle P_4$, is assumed to be zero. Therefore, for the constrained minimization of PI_V, the Lagrangian function is given by:

$$L = \sum_{i=1}^{N} W_V \left(\frac{V_i - V_i^{ss}}{\triangle V_i^{lim}} \right)^2 - \begin{bmatrix} \lambda_1 \\ \lambda_2 \\ \lambda_3 \\ \lambda_4 \end{bmatrix}^T \begin{bmatrix} \triangle P_2 \\ \triangle P_3 \\ \triangle Q_3 \\ \triangle Q_4 \end{bmatrix} \tag{23}$$

The bordered Hessian for the Lagrangian (23) is similar to (13), therefore the FPM is a 9×9 matrix and the SPM is a 10×10 matrix that are to be assessed for positive definiteness. The requirements of positive definiteness lead to the following constraints:

$$1138 V_3^2 \sin^2 (\delta_{12} - \phi_{12}) \quad > \quad 0 \tag{24}$$

$$1.18 \times 10^{-6} V_3^2 V_4^2 \sin^2(\delta_{12} - \phi_{12}) \cos^2(\delta_{24}) \quad > \quad 0 \tag{25}$$

$$\begin{aligned} \sin^2(\delta_{12} - \phi_{12}) V_3^4 V_4^4 \Big(& 0.0011 \sin^2(\delta_{13} - \phi_{13}) \cos^2(\delta_{24}) \cos^2(\delta_{34} - \phi_{34}) \\ & + 0.0011 \cos^2(\delta_{13} - \phi_{13}) \cos^2(\delta_{24}) \sin^2(\delta_{34} - \phi_{34}) - 1.15 \times 10^{-12} \\ & \cos^2(\delta_{13} - \phi_{13}) \cos^2(\delta_{24}) \cos^2(\delta_{34} - \phi_{34}) + 10^{-12} \sin(\delta_{13} - \phi_{13}) \\ & \sin(\delta_{34} - \phi_{34}) \cos(\delta_{13} - \phi_{13}) \cos(\delta_{34} - \phi_{34}) \sin^2(\delta_{24}) - 0.0023 \\ & \sin^2(\delta_{13} - \phi_{13}) \sin(\delta_{34} - \phi_{34}) \cos^3(\delta_{13} - \phi_{13}) \cos(\delta_{34} - \phi_{34}) \cos^2(\delta_{24}) \Big) \quad > \quad 0 \end{aligned} \tag{26}$$

(Equation (A2) in the Appendix) (27)

Assuming V_3 and V_4 to be in the range [0.8, 1.2] and following the same analysis as for the PI_{MVA}, the index PI_V minimization leads to the same angle constraints:

- $-\pi < \delta_{12} < \pi$
- $-\pi + \phi_{13} < \delta_{13} < -\frac{\pi}{2} + \phi_{13}$
- $-\pi + \phi_{34} < \delta_{34} < -\frac{\pi}{2} + \phi_{34}$
- $-\frac{\pi}{2} < \delta_{24} < \frac{\pi}{2}$

C. Cumulative Analysis

The conditions under which the combined metric PI_{cum} for the 3 bus system is guaranteed to be convex are generalized as:

1) The difference of angles between buses connecting different lines in the system should be within a range of, as shown below, where *i* and *j* are buses connecting $Line_{ij}$

$$-\pi + \phi_{ij} < \delta_{ij} < -\pi/2 + \phi_{ij}$$

2) The angle difference across the UPFC should not exceed $\pm\frac{\pi}{2}$
3) The voltages in the system should be within operating range.

These constraints are very mild and apply to most power systems. The conditions under which care must be taken when assuming convexity of the metric are if the system has a small X/R ratio (which affects ϕ_{ij}) or if phase-shifting transformers are heavily utilized.

VI. Sequential Quadratic Programming

Simple gradient descent techniques work well for small nonlinear systems, but become inefficient as the dimension of the search space grows. The nonlinear SQP optimization method is computationally efficient and has been shown to exhibit superlinear convergence for convex search spaces [27]. The SQP method is therefore well-suited for the problem of UPFC powerflow control setting determination for the proposed cumulative index, which is convex over a wide range of system conditions. Interested readers are referred to the companion paper [13] for additional details on the implementation of the SQP method. The following sections describe the SQP algorithm and its application to power systems more fully. In general terms, the optimization problem to be solved is:

$$\begin{aligned} \text{Minimize} \quad & PI_{cum} \\ \text{Subject to} \quad & g_i(x) = 0 \quad i = 1, \ldots, m \\ & h_i(x) \leq 0 \quad i = 1, \ldots, q \end{aligned}$$

where $g(x)$ is the set of powerflow equations, and $h(x)$ is the set of additional inequality constraints governing voltage levels, etc.

VII. Simulation Results

A. Three bus system

Fig. 4 shows the results for the PQ control of the three bus system with the UPFC installed on the line 2 – 3. This figure shows the PQ injections of the UPFC at steady state (dashed line) and at the optimum settings (solid line) provided by the SQP algorithm. Tables I through IV show the bus solutions and line flows before and after UPFC installation, respectively. It can be seen from these results that the voltages and angle differences between buses are within the constraints derived in Section V.

B. 118 bus system

While it is not feasible to analytically determine the angle constraints for systems much larger than the three bus system, the SQP method has been applied to the IEEE 118 bus

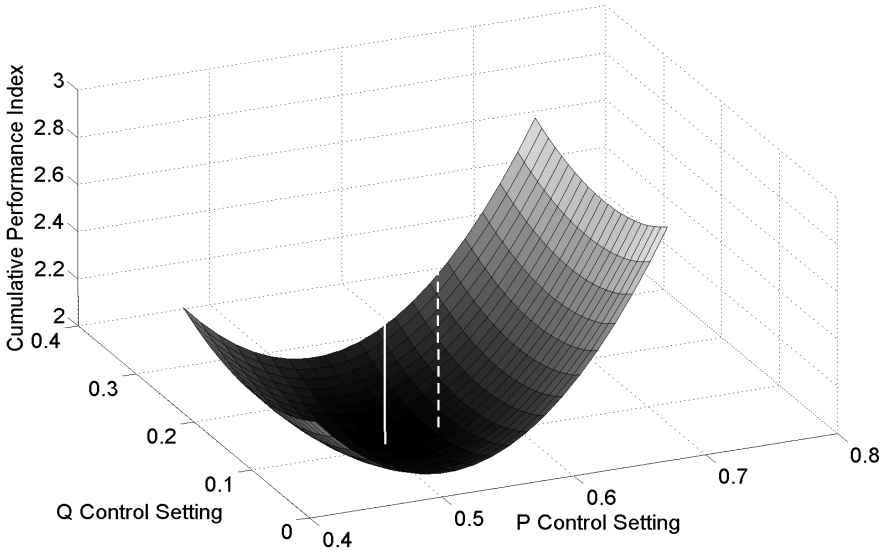

Fig. 4. Control settings for a single placement

TABLE I
BUS SOLUTION BEFORE UPFC INSTALLATION FOR 3 BUS SYSTEM

bus	voltage	angle	Pgen	Qgen	Pload	Qload
1	1.020	0.000	0.708	0.280	0.0	0.0
2	1.000	-0.578	0.500	-0.045	0.0	0.0
3	0.981	-3.639	0.000	0.000	1.2	0.5

system (shown in Fig. 5) under various topologies to illustrate that the search space is convex and that optimal UPFC settings may be found. The SQP method has been applied to find the optimal settings for the cases of one, two, and three UPFCs. Fig. 6 shows the search space for a single UPFC placed on line 26–30 with a line outage of line 23–32. The dashed line indicates the traversal of SQP from an initial value of PI_{cum} = 63.289 at (P, Q) = (1.5182 p.u, -0.2303 p.u) to the minimum PI_{cum}=56.713 at (P, Q) = (2.6705 p.u, 0.7895 p.u), which is indicated by a solid line.

While a simple plot of the two-dimensional search space for a single UPFC convincingly suggests convexity, it is much more challenging to visualize the higher-dimensional search

TABLE II
LINE FLOW BEFORE UPFC INSTALLATION FOR 3 BUS SYSTEM

From (i)	To (j)	P_{ij}	Q_{ij}	S_{ij}	S_{ij}^{max}
1	2	0.039	-0.012	0.144	0.187
1	3	0.670	0.293	0.746	0.857
2	3	0.539	0.094	0.560	0.671

TABLE III
BUS SOLUTION AFTER UPFC INSTALLATION FOR 3 BUS SYSTEM

bus	voltage	angle	Pgen	Qgen	Pload	Qload
1	1.020	0.000	0.708	0.270	0.000	0.000
2	1.000	0.015	0.500	-0.035	0.000	0.000
3	0.982	-3.843	0.000	0.000	1.20	0.500

TABLE IV
LINE FLOW AFTER UPFC INSTALLATION FOR 3 BUS SYSTEM

From (i)	To (j)	P_{ij}	Q_{ij}	S_{ij}	S_{ij}^{max}
1	2	0.003	-0.141	0.141	0.187
1	3	0.705	0.280	0.770	0.857
4	3	0.503	0.106	0.531	0.671

spaces associated with multiple UPFCs in order to indicate convexity. Therefore, Monte Carlo sampling has been conducted for two and three UPFCs to validate that the same optimum is achieved regardless of the initial starting point. The Monte Carlo results indicate that the space is indeed convex and that a global minimum exists and can be identified by the SQP method. Table V gives the results for two UPFCs placed at 5–8 and 26–30 and the same line outage as above for five different test runs. The initial active and reactive powerflow settings are arbitrarily chosen, yet the final settings obtained by SQP are identical. Similarly Table VI gives the results for three UPFCs placed at 5 – 8, 26 – 30 and 38 – 65. In all cases, the final results are the same.

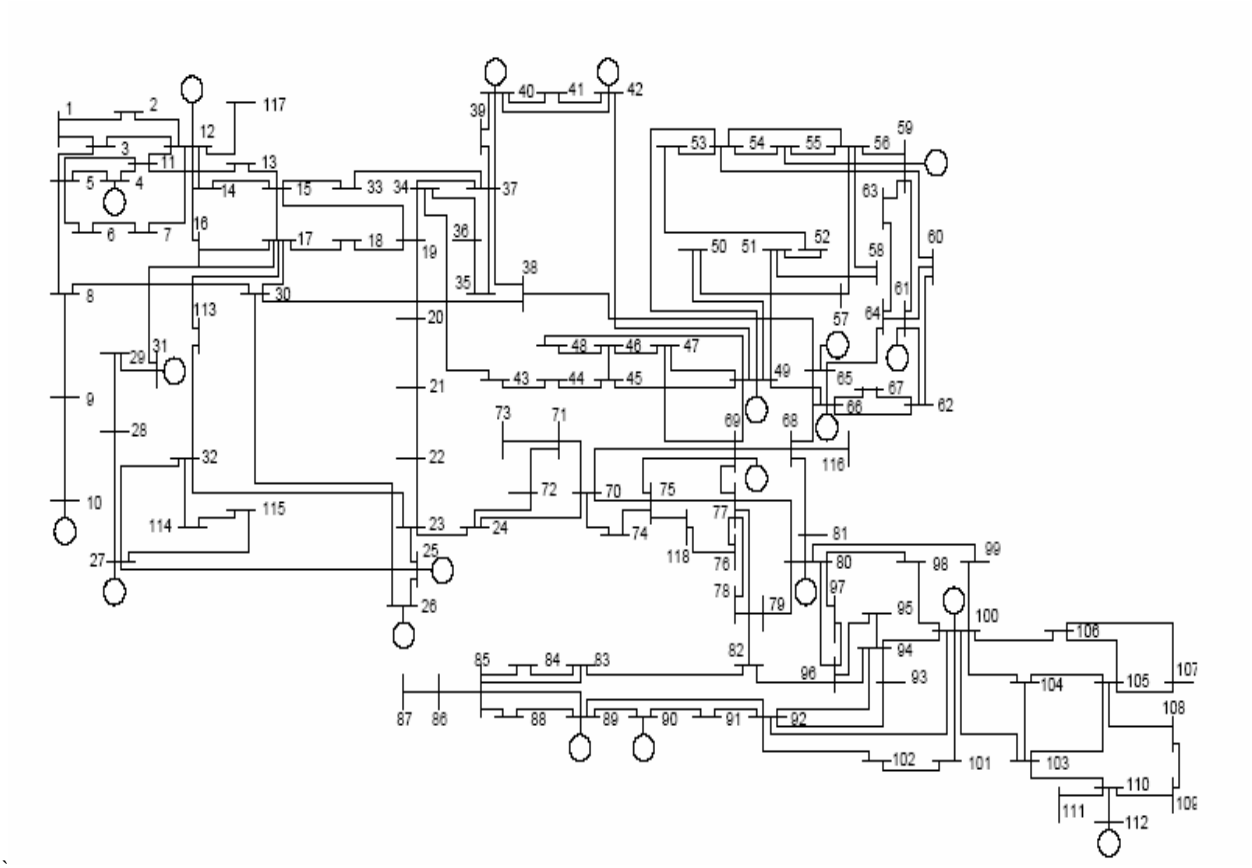

Fig. 5. Line diagram of IEEE 118 bus power system

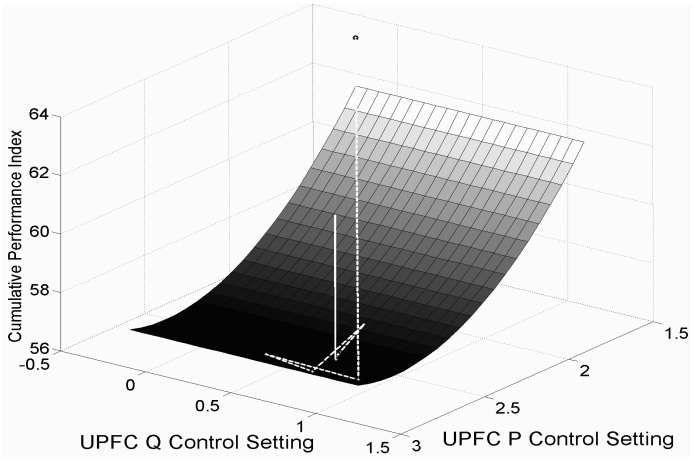

Fig. 6. PQ control for single UPFC placement

VIII. Conclusions

This paper derives the power system operating constraints under which the search space of the cumulative index PI_{cum} is convex leading to the existence of a global minimum. The SQP

TABLE V
MONTE CARLO SAMPLING TEST FOR 2 UPFCS

	Run	1	2	3	4	5
UPFC1	P_{Init}	0.623	0.212	1.082	-0.635	0.781
	Q_{Init}	0.940	-1.007	0.389	0.443	-0.821
UPFC2	P_{Init}	0.799	0.237	-0.131	-0.559	0.569
	Q_{Init}	-0.992	-0.742	0.088	-0.949	-0.265
UPFC1	P_{Final}	-3.323	-3.323	-3.323	-3.323	-3.323
	Q_{Final}	-0.131	-0.131	-0.131	-0.131	-0.131
UPFC2	P_{Final}	2.695	2.695	2.695	2.695	2.695
	Q_{Final}	0.826	0.826	0.826	0.826	0.826
PI_{cum}		56.00	56.00	56.00	56.00	56.00

TABLE VI
MONTE CARLO SAMPLING TEST FOR 3 UPFCS WITH PQ CONTROL

	Run	1	2	3	4	5
UPFC1	P_{Init}	-1.018	0.007	-0.078	0.055	1.863
	Q_{Init}	-0.038	-0.251	0.524	-0.005	-0.807
UPFC2	P_{Init}	-0.182	-0.782	0.889	-1.107	-0.522
	Q_{Init}	1.227	0.48	-0.011	-0.276	0.680
UPFC3	P_{Init}	1.521	0.586	2.309	0.485	0.103
	Q_{Init}	-0.696	0.668	0.913	1.276	-2.364
UPFC1	P_{Final}	-3.317	-3.317	-3.317	-3.317	-3.317
	Q_{Final}	-0.121	-0.120	-0.120	-0.121	-0.121
UPFC2	P_{Final}	2.707	2.707	2.707	2.707	2.707
	Q_{Final}	0.799	0.799	0.799	0.799	0.799
UPFC2	P_{Final}	-1.942	-1.942	-1.942	-1.942	-1.942
	Q_{Final}	-0.106	-0.105	-0.105	-0.105	-0.105
PI_{cum}		55.428	55.428	55.428	55.428	55.428

method is then able to rapidly find the optimal power flow settings of one or more UPFCs. The power system constraints were shown to depend on the transmission lines' X/R ratios, but in most cases the constraints were fairly mild and could be easily met.

ACKNOWLEDGEMENTS

The authors gratefully acknowledge the support of the National Science Foundation under grant CNS-0420869 and the DOE Energy Storage Program through Sandia National Laboratories under BD-0071-D.

REFERENCES

[1] M. S. Bazaraa, H. D. Sherali, and C. M. Shetty, *Nonlinear Programming: Theory and Algorithms*, 2nd ed. Wiley Press, 1993.

[2] S. Boyd and L. Vandenberghe, *Convex Optimization*, 1st ed. Cambridge University Press, 2004.

[3] S. Abraham. (2002, May) National Transmission Grid Study. U. S. Department of Energy. [Online]. Available: http://www.pi.energy.gov/documents/TransmissionGrid.pdf

[4] G. H. Narain and G. Laszlo, *Understanding FACTS: Concepts and Technology of Flexible AC Transmission Systems*. Wiley-IEEE Press, 1999.

[5] E. Acha, C. R. Fuert-Esquivel, H. Ambriz-Perez, and C. Angeles-Camacho, *FACTS: Modelling and Simulation in Power Networks*. John Wiley and Sons, 2004.

[6] V. Azbe, U. Gabrijel, D. Povh, and R. Mihalic, "The energy function of a general multimachine system with a unified power flow controller," in *IEEE Transactions on Power Systems*, vol. 20, 2005, pp. 1478–1485.

[7] S. N. Singh, K. S. Verma, and H. O. Gupta, "Optimal power flow control in open power market using unified power flow controller," in *Power Engineering Society Summer Meeting*, vol. 3, Jul 2001, pp. 1698–1703.

[8] H. C. Leung and T. S. Chung, "Optimal power flow with a versatile FACTS controller by genetic algorithm," in *IEEE Power Engineering Society Winter Meeting*, vol. 4, Jan 2000, pp. 2806–2811.

[9] P. Bhasaputra and W. Ongsakul, "Optimal power flow with multi-type of FACTS devices by hybrid TS/SA approach," in *IEEE International Conference on Industrial Technology*, vol. 1, Dec 2002, pp. 285–290.

[10] H. A. Abdelsalam, G. A. M. Aly, M. Abdelkrim, and K. M. Shebl, "Optimal location of the unified power flow controller in electrical power systems," in *IEEE PES Power Systems Conference and Exposition*, vol. 3, Oct 2004, pp. 1391–1396.

[11] A. Armbruster, M. Gosnell, B. McMillin, and M. L. Crow, "The maximum flow algorithm applied to the placement and distributed steady-state control of UPFCs," in *Proceedings of the 37th Annual North American Power Symposium*, 2005, pp. 77–83.

[12] W. Shao and V. Vittal, "LP-based OPF for corrective FACTS control to relieve overloads and voltage violations," *IEEE Transactions on Power Systems*, vol. 21, no. 4, pp. 1832–1839, 2006.

[13] R. P. Kalyani, M. L. Crow, and D. R. Tauritz, "A nonlinear optimization approach for UPFC power flow control and voltage security," *IEEE Transactions on Power Systems*, 2007, submitted for Publication.

[14] D. J. Gotham and G. T. Heydt, "Power flow control and power flow studies for systems with FACTS devices," *IEEE Transactions on Power Systems*, pp. 60–65, Feb 1998.

[15] I. Musirin and T. K. A. Rahman, "On-line voltage stability based contingency ranking using fast voltage stability index (FVSI)," in *IEEE/PES Asia Pacific Transmission and Distribution Conference and Exhibition*, vol. 2, 2002, pp. 1118 – 1123.

[16] I. Musirin, T. Khawa, and A. Rahman, "Simulation technique for voltage collapse prediction and contingency ranking in power system," in *Student Conference on Research and Development*, 2002, pp. 188 – 191.

[17] J. Zhang, Y. F. Guo, and M. H. Yang, "Assessment of voltage stability for real-time operation," in *IEEE Power India Conference*, 2006, p. 5.

[18] A. Mohamed and G. B. Jasmon, "Voltage contingency selection technique for security assessment," in *IEE Proceedings-Generation, Transmission and Distribution*, vol. 136, 1989, pp. 24 – 28.

[19] P. Kessel and H. Glavitsch, "Estimating the voltage stability of a power system," in *IEEE, Transactions on Power Delivery*, vol. PWRD-1, 1986.

[20] B. Gao, G. K. Morison, and P. Kundur, "Voltage stability evaluation using modal analysis," in *IEEE Transactions on Power Systems*, vol. 7, 1992.

[21] M. Moghavvemi and F. M. Omar, "Technique for contingency monitoring and voltage collapse prediction," in *IEEE Proceeding on Generation, Transmission and Ddistribution*, vol. 145, 1998, pp. 634–640.

[22] G. B. Jasmon and L. H. C. Lee, "New contingency ranking technique incorporating a voltage stability criterion," in *IEE Proceedings-Generation, Transmission and Distribution*, vol. 140, 1993, pp. 87 – 90.

[23] C. T. Chen, *Linear System Theory and Design*. Oxford University Press, 1998.

[24] A. C. Chiang, *Fundamental Methods of Mathematical Economics*. McGraw-Hill, 1984.

[25] D. G. Luenberger, *Linear and Nonlinear Programming*. Adison-Wesley Publishing Company, 1989.

[26] M. L. Crow, *Computational Methods for Electric Power Systems*. CRC Press, 2003.

[27] L. T. Biegler, T. F. Coleman, A. R. Conn, and F. N. Santosa, *Large-Scale Optimization with Applications - Part II: Optimal Design and Control*. Springer-Verlag Inc, 1997.

Appendix

$$
\begin{aligned}
&Re\Bigg\{\sin^2(\delta_{12}-\phi_{12})\,\sin^2(\delta_{24})\,\Bigg\{-1\times10^{-10}\,V_3^4\,V_4^4\cos^2(\delta_{13}-\phi_{13})\sin^2(\delta_{34}-\phi_{34})\sin(\delta_{13}-\phi_{13})\\
&-3.07\times10^{-11}\,V_3^5\,V_4^4\,\cos^2(\delta_{13}-\phi_{13})\sin^2(\delta_{34}-\phi_{34})\cos(\delta_{34}-\phi_{34})-1.2\times10^{-10}V_3^3\,V_4^5\\
&\cos^2(\delta_{13}-\phi_{13})\sin^2(\delta_{34}-\phi_{34})\sin(\delta_{13}-\phi_{13})-1.15\times10^{-10}\,V_3^5\,V_4^2\,\cos^2(\delta_{13}-\phi_{13})\cos^2(\delta_{34}-\phi_{34})\\
&\sin(\delta_{13}-\phi_{13})-1.65\times10^{-10}\,V_3^2\,V_4^5\,\cos^2(\delta_{13}-\phi_{13})\cos^2(\delta_{34}-\phi_{34})\sin(\delta_{34}-\phi_{34})\\
&-1.8\times10^{-10}\,V_3^6\,V_4^3\,\sin^2(\delta_{13}-\phi_{13})\sin^3(\delta_{34}-\phi_{34})+1.98\times10^{-10}\,V_3^2\,V_4^5\,\cos(\delta_{24})\\
&\sin^2(\delta_{34}-\phi_{34})\cos^2(\delta_{34}-\phi_{34})-1.66\times10^{-10}\,V_3^4\,V_4^5\,\cos^2(\delta_{13}-\phi_{13})\sin^2(\delta_{34}-\phi_{34})\cos(\delta_{34}-\phi_{34})\\
&+2.7\times10^{-10}\,V_3\,V_4^3\,\cos^2(\delta_{13}-\phi_{13})\sin^2(\delta_{34}-\phi_{34})-6.90\times10^{-11}\,\sin^3(\delta_{13}-\phi_{13})\\
&\sin(\delta_{34}-\phi_{34})\cos^2(\delta_{34}-\phi_{34})+1.47\times10^{-10}\,V_3^4\,V_4^5\,\cos^2(\delta_{13}-\phi_{13})\cos^2(\delta_{34}-\phi_{34})\,\sin^4(\delta_{13}-\phi_{13})\\
&-1.6\times10^{-10}\,V_3^3\,V_4^4\,\sin^2(\delta_{13}-\phi_{13})\sin^2(\delta_{34}-\phi_{34})\,\cos(\delta_{13}-\phi_{13})-4.15\times10^{-11}\\
&V_3^4\,V_4^6\,\cos^2(\delta_{13}-\phi_{13})\,\cos^4(\delta_{34}-\phi_{34})\,\sin(\delta_{34}-\phi_{34})-1.4\times10^{-10}\,V_3^2\,V_4^4\,\sin^4(\delta_{13}-\phi_{13})\,\sin^2(\delta_{34}-\phi_{34})\\
&\cos(\delta_{13}-\phi_{13})-4.73\times10^{-10}\,V_3^5\,V_4^6\,\sin^2(\delta_{13}-\phi_{13})\,\sin^2(\delta_{34}-\phi_{34})\cos(\delta_{13}-\phi_{13})-6.40\times10^{-11}\\
&V_3^5\,V_4^3\,\sin^4(\delta_{13}-\phi_{13})\sin(\delta_{34}-\phi_{34})\cos(\delta_{13}-\phi_{13})\cos(\delta_{34}-\phi_{34})-3\times10^{-10}\,V_3^5\,V_4\\
&\sin(\delta_{13}-\phi_{13})\sin^2(\delta_{34}-\phi_{34})\cos(\delta_{13}-\phi_{13})-4.15\times10^{-11}\,V_3^2\,V_4^3\,\sin^2(\delta_{13}-\phi_{13})\,\cos^3(\delta_{34}-\phi_{34})\\
&-2.03\times10^{-10}\,V_3^3\,V_4^2\,\cos^2(\delta_{13}-\phi_{13})\,\cos^2(\delta_{34}-\phi_{34})-8\times10^{-10}\,V_3^4\,V_4^5\,\cos^2(\delta_{13}-\phi_{13})\\
&\cos^2(\delta_{34}-\phi_{34})\,\sin(\delta_{13}-\phi_{13})\sin^4(\delta_{34}-\phi_{34})+2\times10^{-11}\,V_3^2\,V_4^4\,\sin^4(\delta_{13}-\phi_{13})\sin^2(\delta_{34}-\phi_{34})\\
&-2.7\times10^{-10}\,V_3^4\,V_4^5\,\sin^4(\delta_{13}-\phi_{13})\cos^2(\delta_{34}-\phi_{34})\,\cos(\delta_{13}-\phi_{13})\,+2.04\times10^{-12}\\
&V_3^2\,V_4^4\,\sin^3(\delta_{13}-\phi_{13})\sin^2(\delta_{24})\,\cos(\delta_{24})\cos(\delta_{34}-\phi_{34})-5.04\times10^{-13}\,V_3^3\,V_4^2\\
&\sin^2(\delta_{13}-\phi_{13})\,\sin^3(\delta_{34}-\phi_{34})\,\cos(\delta_{24})\,\sin^2(\delta_{13}-\phi_{13})\,\sin^2(\delta_{34}-\phi_{34})\,\cos(\delta_{34}-\phi_{34})\\
&-3\times10^{-10}\,V_3^4\,V_4^4\,\sin^2(\delta_{13}-\phi_{13})\,\sin^3(\delta_{34}-\phi_{34})-1\times10^{-10}\,V_3^2\,V_4^3\,\cos^4(\delta_{13}-\phi_{13})\\
&\sin^2(\delta_{34}-\phi_{34})-1.2\times10^{-9}\,V_3\,V_4^4\,\sin^3(\delta_{13}-\phi_{13})\,\sin^2(\delta_{34}-\phi_{34})-3\times10^{-10}\\
&V_3^3\,V_4^5\,\sin^2(\delta_{13}-\phi_{13})\,\sin^4(\delta_{34}-\phi_{34})-1.47\times10^{-9}\,V_3^2\,V_4^6\,\sin^2(\delta_{13}-\phi_{13})\\
&\sin^2(\delta_{34}-\phi_{34})\cos(\delta_{13}-\phi_{13})-1.6\times10^{-10}\,V_3^4\,V_4^3\,\cos^3(\delta_{13}-\phi_{13})\,\sin^2(\delta_{34}-\phi_{34})\\
&-1.47\times10^{-9}\,V_3\,V_4^2\,\sin^2(\delta_{13}-\phi_{13})\sin^2(\delta_{34}-\phi_{34})\cos(\delta_{34}-\phi_{34})\\
&-1.6\times10^{-10}\,\cos^2(\delta_{13}-\phi_{13})\sin^2(\delta_{34}-\phi_{34})-4.15\times10^{-11}\,V_3^3\,V_4^3\,\cos^4(\delta_{13}-\phi_{13})\\
&\sin^2(\delta_{34}-\phi_{34})\,\cos(\delta_{34}-\phi_{34})-4.15\times10^{-10}\,V_3^4\,V_4^4\,\cos^2(\delta_{13}-\phi_{13})\,(\cos(\delta_{24}))\,\sin^3(\delta_{34}-\phi_{34})\\
&+2.30\times10^{-10}\,V_3^5\,V_4^5\,\cos^2(\delta_{13}-\phi_{13})\cos(\delta_{24})\,\cos^4(\delta_{34}-\phi_{34})-1.15\times10^{-10}V_3^3\,V_4^2\\
&\cos^2(\delta_{13}-\phi_{13})\,\cos^3(\delta_{34}-\phi_{34})-3.20\times10^{-11}\,V_3^3\,V_4^3\,\sin^2(\delta_{13}-\phi_{13})\sin^2(\delta_{34}-\phi_{34})\cos(\delta_{34}-\phi_{34})\\
&+2\times10^{-10}\,V_3^2\,V_4^4\,\sin^2(\delta_{13}-\phi_{13})\sin^2(\delta_{34}-\phi_{34})\cos^2(\delta_{34}-\phi_{34})-7\times10^{-10}V_3^3\,V_4^3\\
&\sin^2(\delta_{13}-\phi_{13})\,\sin^2(\delta_{34}-\phi_{34})-1\times10^{-10}\,V_3^2\,V_4^4\,\sin^2(\delta_{13}-\phi_{13})\,\cos^2(\delta_{13}-\phi_{13})\sin^2(\delta_{34}-\phi_{34})\\
&-7.35\times10^{-11}\,V_3\,V_4^4\,\sin^2(\delta_{13}-\phi_{13})\,\cos^4(\delta_{34}-\phi_{34})\,\cos(\delta_{13}-\phi_{13})\\
&-4.15\times10^{-11}V_3^3\,V_4^2\,\sin^4(\delta_{13}-\phi_{13})\,\sin(\delta_{34}-\phi_{34})\,\cos(\delta_{34}-\phi_{34})-4\times10^{-10}\,V_3^5\,V_4^4\,\sin^4(\delta_{13}-\phi_{13})\\
&\cos^2(\delta_{34}-\phi_{34})\,\sin(\delta_{34}-\phi_{34})-1.6\times10^{-9}\,V_3^6\,V_4^6\,\sin^2(\delta_{13}-\phi_{13})\,\cos^2(\delta_{34}-\phi_{34})\sin(\delta_{34}-\phi_{34})\Bigg\}\Bigg\}>0
\end{aligned}
\tag{A1}
$$

$$
\begin{aligned}
&Re\Bigg(\sin^2(\delta_{12}-\phi_{12})\Bigg(1.03\times10^{-10}\,{V_4}^5\sin^2(\delta_{24})\;{V_3}^5\;\sin^2(\delta_{13}-\phi_{13})\;\sin(\delta_{34}-\phi_{34})\\
&\cos^2(\delta_{34}-\phi_{34})\;\cos(\delta_{13}-\phi_{13})+1.13\times10^{-10}\,{V_3}^4\;\sin^4(\delta_{13}-\phi_{13})\;{V_4}^4\cos^2(\delta_{24})\\
&\cos^2(\delta_{34}-\phi_{34})-1.15\times10^{-10}\,{V_3}^4\sin^3(\delta_{13}-\phi_{13})\;{V_4}^4\;\cos^2(\delta_{24})\;\sin^2(\delta_{34}-\phi_{34})\\
&-1.15\times10^{-10}\,{V_3}^5\cos^2(\delta_{13}-\phi_{13})\,{V_4}^5\sin^2(\delta_{24})\;\sin^3(\delta_{34}-\phi_{34})\\
&-1.15\times10^{-10}\;\sin^2(\delta_{12}-\phi_{12})\,{V_3}^4\cos^3(\delta_{13}-\phi_{13})\\
&{V_4}^4\;\cos^2(\delta_{24})-4\times10^{-10}\,{V_3}^5\cos(\delta_{13}-\phi_{13})\,{V_4}^5\;\cos(\delta_{34}-\phi_{34})\;\sin^2(\delta_{24})\\
&\sin^2(\delta_{34}-\phi_{34})\;\sin(\delta_{13}-\phi_{13})+10^{-10}{V_3}^4\sin^3(\delta_{13}-\phi_{13})\;{V_4}^5\;\sin^2(\delta_{34}-\phi_{34})\cos(\delta_{34}-\phi_{34})\\
&-8.04\times10^{-11}\,{V_3}^4\;\sin^3(\delta_{13}-\phi_{13})\,{V_4}^5\;\sin^2(\delta_{24})\;\cos^2(\delta_{34}-\phi_{34})-1.15\times10^{-10}{V_3}^4\\
&\sin^2(\delta_{13}-\phi_{13})\;{V_4}^5\;\cos^2(\delta_{24})\;\cos^3(\delta_{34}-\phi_{34})+1.15\times10^{-10}{V_3}^4\sin^2(\delta_{13}-\phi_{13})\;{V_4}^4\\
&\cos^2(\delta_{24})\cos^2(\delta_{34}-\phi_{34})\;\cos^2(\delta_{13}-\phi_{13})-3.45\times10^{-11}\,{V_3}^5\;\sin^2(\delta_{13}-\phi_{13})\;{V_4}^4\;\cos^2(\delta_{24})\\
&\cos^2(\delta_{34}-\phi_{34})\cos(\delta_{13}-\phi_{13})+3.45\times10^{-10}\,{V_3}^5\;\sin^2(\delta_{13}-\phi_{13})\;{V_4}^5\cos^2(\delta_{24})\\
&\cos^2(\delta_{34}-\phi_{34})\sin^2(\delta_{34}-\phi_{34})-1.15\times10^{-11}\,{V_3}^5\sin^3(\delta_{13}-\phi_{13})\\
&{V_4}^4\cos^2(\delta_{24})\sin(\delta_{34}-\phi_{34})\cos(\delta_{34}-\phi_{34})-3.45\times10^{-11}\,{V_3}^5\left(\sin(\delta_{13}-\phi_{13})\right)^2{V_4}^5\;\cos^2(\delta_{24})\\
&\sin^2(\delta_{34}-\phi_{34})\cos(\delta_{34}-\phi_{34})+3.45\times10^{-10}\,{V_3}^4\sin^2(\delta_{13}-\phi_{13})\;{V_4}^5\cos^2(\delta_{24})\\
&\sin^2(\delta_{34}-\phi_{34})\;\cos(\delta_{34}-\phi_{34})\cos(\delta_{13}-\phi_{13})\\
&+4.58\times10^{-11}\;\left(\sin(\delta_{12}-\phi_{12})\right)^2{V_3}^6\cos^2(\delta_{13}-\phi_{13}){V_4}^4\left(\sin(\delta_{24})\right)^2\left(\sin(\delta_{34}-\phi_{34})\right)^2\\
&-2.3\times10^{-11}\,{V_3}^5\cos^2(\delta_{13}-\phi_{13}){V_4}^5\left(\cos(\delta_{24})\right)^2\left(\cos(\delta_{34}-\phi_{34})\right)^3-5.63\times10^{-10}\\
&{V_3}^6\cos(\delta_{13}-\phi_{13})\,{V_4}^4\left(\cos(\delta_{24})\right)^2\left(\cos(\delta_{34}-\phi_{34})\right)^2+1.15\times10^{-10}\;\sin^2(\delta_{12}-\phi_{12})\,{V_3}^6\\
&\cos^2(\delta_{13}-\phi_{13}){V_4}^4\;\cos^2(\delta_{24})\sin(\delta_{34}-\phi_{34})\cos(\delta_{34}-\phi_{34})+1.03\times10^{-10}\,{V_3}^5\;\sin^2(\delta_{13}-\phi_{13})\,{V_4}^5\\
&\sin^2(\delta_{24})\;\sin^2(\delta_{34}-\phi_{34})(\cos(\delta_{34}-\phi_{34}))^2-1.15\times10^{-11}\,{V_3}^5\;\sin^2(\delta_{13}-\phi_{13})^2\,{V_4}^5\left(\cos(\delta_{24})\right)^2\\
&\cos^3(\delta_{34}-\phi_{34})+1.15\times10^{-10}\;\sin^2(\delta_{12}-\phi_{12})\,{V_3}^6\;\sin^2(\delta_{13}-\phi_{13})\,{V_4}^4\;\cos^2(\delta_{24})\\
&\sin(\delta_{34}-\phi_{34})\cos(\delta_{34}-\phi_{34})-10^{-10}\,{V_3}^4\sin(\delta_{13}-\phi_{13})\,{V_4}^5\left(\sin(\delta_{24})\right)^2\;\cos^3(\delta_{34}-\phi_{34})\\
&\cos(\delta_{13}-\phi_{13})-1.15\times10^{-10}\,{V_3}^5\sin^2(\delta_{13}-\phi_{13})\;{V_4}^5\;\sin^2(\delta_{24})\;\cos^2(\delta_{34}-\phi_{34})\\
&\sin(\delta_{34}-\phi_{34})+2.3\times10^{-13}\,{V_3}^4\cos^2(\delta_{13}-\phi_{13}){V_4}^7\;\sin^3(\delta_{24})\;\sin^2(\delta_{34}-\phi_{34})\;\cos^2(\delta_{34}-\phi_{34})\\
&+1.13\times10^{-8}\,{V_3}^8\cos^2(\delta_{13}-\phi_{13}){V_4}^4\;\cos^2(\delta_{24})\;\cos^3(\delta_{34}-\phi_{34})\;\sin(\delta_{34}-\phi_{34})\\
&-2.27\times10^{-9}\,{V_3}^6\cos^2(\delta_{13}-\phi_{13}){V_4}^5\;\cos^2(\delta_{24})\;\cos^3(\delta_{34}-\phi_{34})\sin^2(\delta_{13}-\phi_{13})\\
&+1.13\times10^{-8}\,{V_3}^6\cos^2(\delta_{13}-\phi_{13}){V_4}^6\;\cos^4(\delta_{34}-\phi_{34})\;\cos^2(\delta_{24})-1.13\times10^{-8}\,{V_3}^5\\
&\cos^3(\delta_{13}-\phi_{13})\;{V_4}^6\;\cos^2(\delta_{34}-\phi_{34})\;\cos^2(\delta_{24})^2-9.07\times10^{-9}\;\sin^2(\delta_{13}-\phi_{13})\;{V_3}^5{V_4}^7\cos^2(\delta_{24})\\
&\cos^3(\delta_{34}-\phi_{34})-7.72\times10^{-9}\,{V_3}^7\;\cos^2(\delta_{13}-\phi_{13})\;{V_4}^4\cos^2(\delta_{24})\\
&\cos^3(\delta_{34}-\phi_{34})\Bigg)\Bigg)>0
\end{aligned}
\tag{A2}
$$

PAPER 2

A Nonlinear Optimization Approach for UPFC Power Flow Control and Voltage Security

R P. Kalyani, *Student Member, IEEE*, M. L. Crow, *Senior Member, IEEE*, and D. R. Tauritz, *Member, IEEE*

ABSTRACT

This paper proposes a new nonlinear optimization algorithm for calculating the long term control settings of one or more UPFCs in a power system across the set of all possible single line outages to relieve overloads and maintain voltage security. Active and reactive power performance indices are employed to guide the corrective UPFC control. The proposed method has been implemented and compares favorably with linear programming (LP) based optimization for the same constraints. The method is tested on the IEEE 39 bus system and the IEEE 118 bus system.

***Index Terms*— FACTS, UPFC, Long Term Control, Performance Index, Sequential Quadratic Programming**

I. INTRODUCTION

The Unified Power Flow Controller (UPFC) is a device that can simultaneously control the voltage magnitudes at the sending end and the active and reactive power flows at the receiving end bus. This controller provides flexibility for AC power transmission control and reacts nearly instantaneously to new active and reactive demands to enhance the transmission capacity of the bulk power system. Given the fast acting control possible with the UPFC, it is desirable to utilize it to control power flows in order to relieve line overloads and transmission

Kalyani and Crow are with the Electrical & Computer Engineering Department, University of Missouri-Rolla, Tauritz is with the Computer Science Department, University of Missouri-Rolla, Rolla, MO 65409-0810

congestion as well as provide voltage support. To accomplish this goal requires that the UPFC settings be chosen according to some quantitative measure or objective function over the set of system topologies, loading and generation profiles of interest.

Most of the Flexible AC Transmission System (FACTS) control setting algorithms described in the literature have been applied to a power system for a particular set topology, load, and generation profile [1]–[5]. The described methods were applied to static systems and did not consider the effect of topology changes due to line outages. To date, only a few authors have developed algorithms for improving the transmission line loading profile over the entire set of possible single line contingencies [6], [7]. In [6], a transportation scheduling algorithm (the maxflow algorithm) is proposed to determine the UPFC powerflow control settings to decrease overloads and improve loadability over all system contingency conditions. This method has the advantage of being computationally efficient and suitable for distributed computing, but does not consider voltage security, nor is it guaranteed to provide an optimal solution. In [7], a Linear Programming (LP) based OPF is proposed to relieve overloads and alleviate voltage violations. This approach showed promising results, but does not guarantee an optimal solution, especially for large search spaces for multiple UPFCs. In this paper, the Sequential Quadratic Programming (SQP) method is proposed for the same problem as [6], [7], but it will be shown to provide improved results.

Optimization problems with equality and inequality constraints have been solved successfully by both linear programming and nonlinear programming (NLP) methods. NLP approaches include iterative methods such as quadratic programming and Newton methods. The advantage of NLP methods over LP methods is that NLP methods can explicitly handle nonlinearities and guarantee a global minimum under certain system conditions such as search space convexity. The primary drawback of NLP methods is that they tend to be more computationally intensive than LP methods and therefore time-consuming. However, the SQP method proposed in this paper will be shown to not only produce more accurate results than LP methods, but will also be shown to do so in a computationally efficient manner.

A power system is an inherently nonlinear system. Thus a nonlinear optimization will usually provide better results over a wider range of operating conditions. As discussed in

[8], any method tailored to the characteristics of the system's search space can be expected to perform the best. Considering the system nonlinearities, an NLP algorithm is therefore proposed to determine the powerflow control setting of the UPFCs. This NLP algorithm minimizes an objective function based on classical performance indices employed in the literature for contingency screening and voltage security.

The nonlinear SQP method combines the advantages of the Newton method with those of standardized quadratic programming. At each iteration of the Newton method, SQP solves a corresponding quadratic subproblem. By generalizing the quadratic subproblem, inequality constraints and limitations on the state variables can be handled by SQP. In addition, it has been shown that SQP methods will reach the global minimum of a convex objective function in superlinear time leading to computational efficiency [9].

II. The UPFC Power Injection Model

The UPFC is a device that is capable of simultaneously controlling voltage magnitudes and active and reactive power flows. In this paper, the active and reactive power of the device are controlled to minimize overloading along transmission corridors across the set of possible single line contingencies and to maintain voltage security. Fig. 1 shows the power injection model of a lossless UPFC utilized in the algorithm development and simulations results [10].

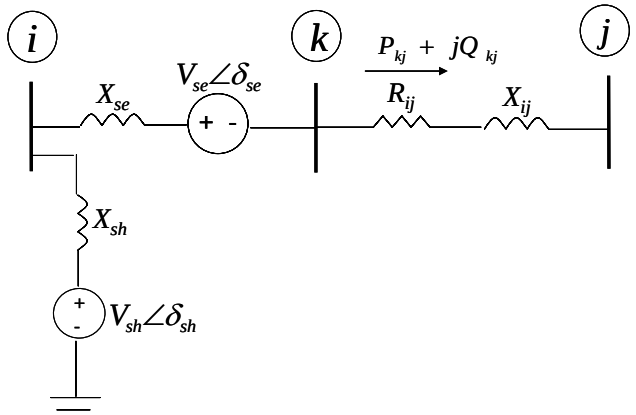

Fig. 1. Power injection model of UPFC

To incorporate the UPFC into a powerflow program, the transmission line must be modified to accurately represent the UPFC characteristics. To install a UPFC at bus i on transmission

line $i-j$, a fictitious bus k is introduced between buses i and j, as shown in Fig. 1. This model is consistent with the UPFC model for power flow control proposed in [7] where the sending end bus is modeled as a "PV" bus and the receiving end is modeled as a "PQ" bus. The UPFC is assumed to be capable of altering the power flow through line $i-j$ by $\pm$ 20% of the original line capacity, S_{ij}^{max}. The equations governing the UPFC are:

$$P_{se} = \frac{V_{se}}{X_{se}}\left[V_j \sin\left(\delta_{se}-\delta_j\right) - V_i \sin\left(\delta_{se}-\delta_i\right)\right] \quad (1)$$

$$Q_{se} = \frac{V_{se}}{X_{se}}\left[V_i \sin\left(\delta_{se}-\delta_i\right) - V_j \cos\left(\delta_{se}-\delta_j\right) - V_{se}\right] \quad (2)$$

$$P_{sh} = -V_{sh}V_i \sin(\delta_{sh}-\delta_i)/X_{sh} \quad (3)$$

$$Q_{sh} = V_{sh}\left[V_i \cos(\delta_{sh}-\delta_i) - V_{sh}\right]/X_{sh} \quad (4)$$

$$S_{kj} = P_{kj} + jQ_{kj} = \bar{V}_k\left(\frac{\bar{V}_k - \bar{V}_j}{Z_{ij}}\right)^* \quad (5)$$

$$\bar{V}_k = \bar{V}_i + \bar{V}_{se} \quad (6)$$

$$I_{sh} = \left(\frac{Q_{sh}}{\bar{V}_i}\right)^* \quad (7)$$

where $\bar{V}_i = V_i\angle\theta_i,\ \bar{V}_k = V_k\angle\theta_k,$ and $\bar{V}_{se} = V_{se}\angle\theta_{se}$.

III. UPFC Objective Function

To determine the optimal powerflow setting for the UPFC, it is necessary to define an objective function that measures the "goodness" of a particular setting. In this paper, the objective function is derived from power flow constraints and voltage security. Therefore, two performance indices, which provide measures of line loadability and bus voltage violations respectively, are utilized for determining the long term UPFC settings in this paper [11], [12]. This approach is consistent with contingency screening approaches that maintain two separate ranking lists for line overloads and voltage violations since contingencies causing line overloads do not necessarily cause bus voltage violations and vice versa [11], [13]–[21].

A. Power Flow Performance Index

The power flow performance index (PI_{MVA}) provides a measure of the loadability of the system. It is large if any lines are overloaded and small if all loadability conditions are satisfied.

A good UPFC powerflow setting is one that minimizes the number of overloaded lines and furthermore "flattens" the line loading profile by reducing the powerflows on heavily loaded lines and increasing the flow on lightly loaded lines. The PI_{MVA} provides such a measure:

$$PI_{MVA} = \sum_{all\,lines} \left(\frac{S_{ij}}{S_{ij}^{max}} \right)^2 \tag{8}$$

where

S_{ij} apparent power flow on line $i-j$ for each SLC

S_{ij}^{max} maximum power flow on line $i-j$

Minimizing PI_{MVA} effectively minimizes all line overloads in the systen since higher overloads incur heavier penalties than lower overloads. Furthermore, minimizing PI_{MVA} produces better utilization of all lines in the system because as overloads are minimized, lightly loaded lines are more heavily utilized. The optimal UPFC power flow control setting is one in which PI_{MVA} is minimized.

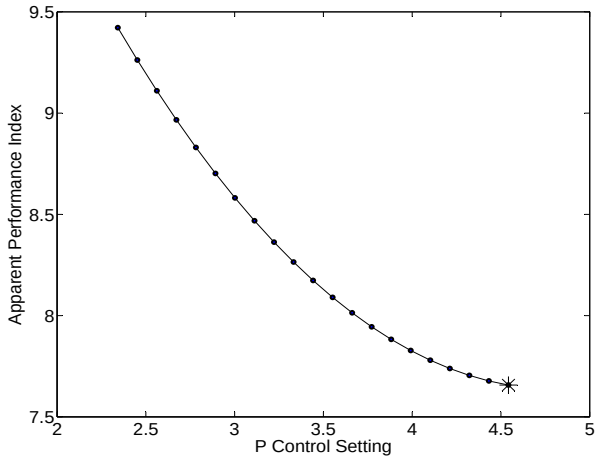

Fig. 2. PI_{MVA} space for a single UPFC placement (13-14) and SLC (4-5)

Fig. 2 shows the PI_{MVA} metric space for a random single line contingency (SLC) on line 4–5 in the IEEE 39 bus test system with a single UPFC placed randomly on line 13–14. The steady-state powerflow on this line is 3.53 p.u. The UPFC can adjust the powerflow on the line by $\pm$ 20% of the line rating S_{ij}^{max}. This line has a rating of 5.5 p.u., therefore the UPFC can adjust the powerflow on the line by 1.1 p.u. (20% of 5.5 p.u.). Thus, the range

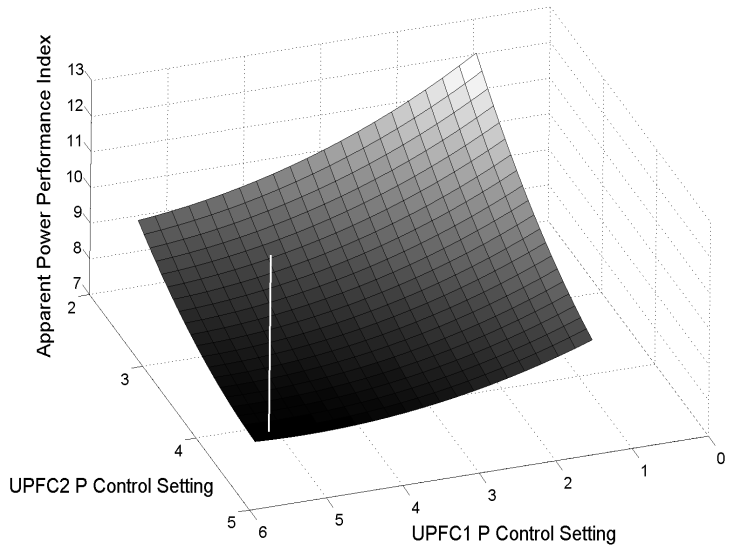

Fig. 3. PI_{MVA} space for two UPFC placements (13-14, 2-3) for SLC (4-5)

of allowable active powerflow settings for the UPFC on this line is between 2.43 and 4.63 p.u. For this particular UPFC placement and line outage, the optimal UPFC powerflow control setting determined by minimizing PI_{MVA} is 4.54 p.u., which falls in the acceptable range and is shown as the '*' in Fig. 2. Note that the index PI_{MVA} leads to a smooth convex surface on which a minimum value can be easily obtained.

Similarly, Fig. 3 shows the PI_{MVA} space for the two (random) UPFC placements 2–3 and 4–14 over a range of control settings for the same SLC 4–5. The vertical line in the figure indicates the minimum PI_{MVA} value for the best UPFC power flow control settings [5.36 p.u., 4.44 p.u.] of the two UPFCs respectively. Note that, even for two UPFCs, the index space is convex and smooth. While this paper focuses on the implementation of the method, the companion paper [22] establishes the power system boundaries and constraints under which the PI_{MVA} surface is guaranteed to be convex.

B. Voltage Security Index

In addition to overloads, voltage security is also of primary concern in a power system. In order to maintain voltage security, power system operators require information regarding the proximity of voltage instability to the current operating point. In the literature, several voltage

performance indices have been proposed to find the critical bus which causes voltage instability in the event of a line outage [14]–[20]. Recent work has shown that all of these indices provide consistent results, identifying the same critical buses in post contingency conditions [23]. Of the indices analyzed in [23], the voltage performance index (PI_V), first proposed by [14], [21], has a convex search space similar to the power flow index PI_{MVA} and will therefore be used as the voltage security index in this paper. The PI_V is given by:

$$PI_V = W_V \sum_{i=1}^{N} \left(\frac{V_i - V_i^{ss}}{\triangle V_i^{lim}} \right)^2 \tag{9}$$

where

V_i	voltage magnitude at bus *i*
V_i^{ss}	voltage magnitude at bus *i* in steady state
V_i^{lim}	voltage deviation limit, above which voltage deviations are unacceptable
N	number of buses
W_V	nonnegative weighting factor

Fig. 4 shows the PI_V space for the same contingency (line 4–5) in the 39 bus test system with the UPFC placed on line 13–14 with the optimal reactive power setting (1.54 p.u.). Note that this surface is also convex. The allowable reactive flow control settings for the UPFC are in the range of $\pm\sqrt{(S_{ij}^{max})^2 - P_{set}^2}$ where P_{set} is the active power control setting. The active and reactive power flow settings are always constrained such that the apparent power on the line is less than or equal to the line rating S_{ij}^{max}.

The PI_V space for two UPFC placements (2–3 and 13–14) for the same SLC (4–5) is shown in Fig. 5. The control settings which provide the optimal voltage security margin in the event of a SLC are 2.64 p.u. for UPFC placement 2–3 and 1.21 p.u. for the UPFC on line 13–14.

C. The Cumulative Performance Index

Since both the PI_{MVA} and PI_V indices are convex functions, a nonnegative weighted sum of these two functions will also result in a convex function [24] that can be minimized by the nonlinear SQP method. The indices PI_{MVA} and PI_V are therefore combined to provide

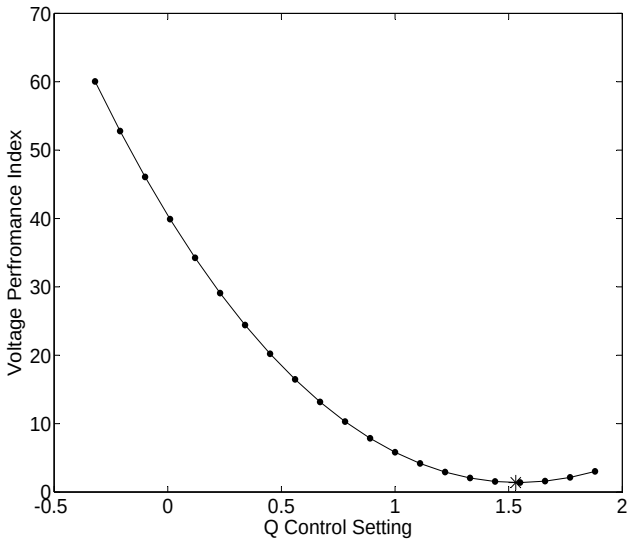

Fig. 4. PI_V space for a single UPFC placement (13–14) for SLC (4–5)

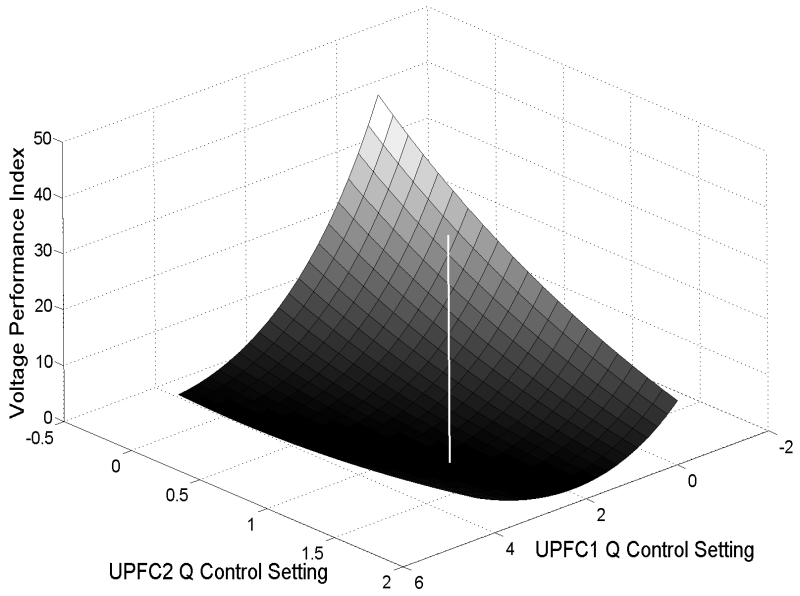

Fig. 5. PI_V curvature for two UPFC placements (13–14, 2–3) for SLC (4–5)

a new convex Cumulative Performance Index (PI_{cum}). The convex space resulting from this combination is used to find the minimum of the combined fitness function which provides simultaneously, the active and reactive power flow control setting with minimum overloading

and the best voltage security. Fig 6 shows the P and Q control for the same line outage 4–5 for a UPFC placement on line 13–14 in the IEEE 39 bus system. The simultaneous control of active and reactive power produces the minimum value of the objective function as shown by the vertical line in Fig. 6.

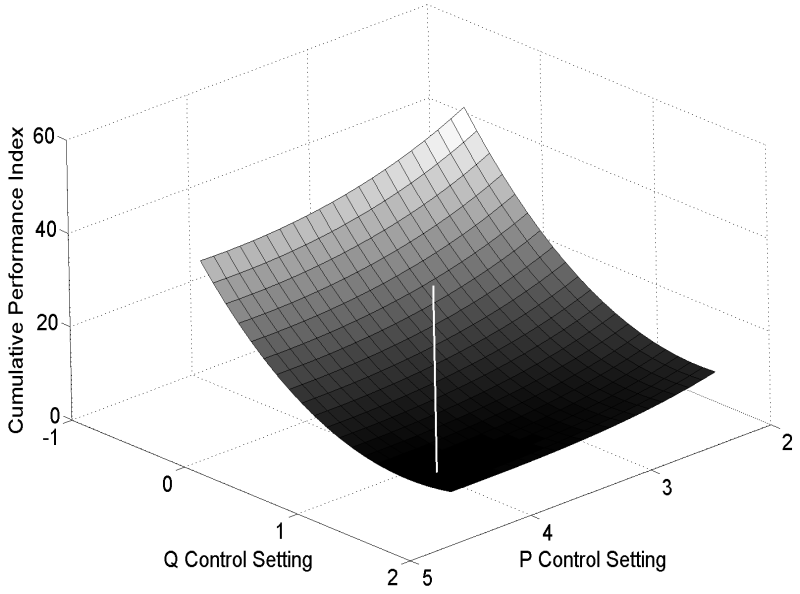

Fig. 6. PI_{cum} curvature for a single UPFC placement (13–14) for SLC (4–5)

The nonlinear optimization problem for the settings of one or more UPFCs constrained by powerflow equations can be formulated as:

$$\text{Minimize } PI_{cum} = \sum_{all\ lines} \left(\frac{S_{ij}}{S_{ij}^{max}}\right)^2 + W_V \sum_{i=1}^{N} \left(\frac{V_i - V_i^{ss}}{\triangle V_i^{lim}}\right)^2 \tag{10}$$

Equality constraints:

$$0 = \triangle P_i - \sum_{j=1}^{N} V_i V_j Y_{ij} \cos(\theta_i - \theta_j - \phi_{ij})$$

$$0 = \triangle Q_i - \sum_{j=1}^{N} V_i V_j Y_{ij} \sin(\theta_i - \theta_j - \phi_{ij})$$

for *i=1,...,N* and *j=1,...,N*

Inequality constraints:

$$P_i^{min} \leq P_i \leq P_i^{max}$$

$$Q_i^{min} \leq Q_i \leq Q_i^{max}$$

$$V_i^{min} \leq V_i \leq V_i^{max}$$

UPFC constraints:

$$\sqrt{P_{SET}^2 + Q_{SET}^2} \leq S_{ij}^{max}$$

where

P_i	Active power generation at bus *i*
Q_i	Reactive power generation at bus *i*
P_i^{min}	Minimum active power generation at bus *i*
P_i^{max}	Maximum active power generation at bus *i*
Q_i^{min}	Minimum reactive power generation at bus *i*
Q_i^{min}	Maximum reactive power generation at bus *i*
V_i	Voltage magnitude at bus *i*
V_i^{min},V_i^{max}	Min and Max voltage magnitude at bus *i*
V_j	Voltage magnitude at bus *j*
Y_{ij}	Magnitude of the (i, j) element of the admittance matrix
ϕ_{ij}	Angle of the (i, j) element of the admittance matrix
S_{ij}^{max}	Maximum apparent power flow on the line *i-j*
P_{set},Q_{set}	Active and reactive settings of the UPFC

IV. Sequential Quadratic Programming

Simple gradient descent techniques work well for small nonlinear systems, but become inefficient as the dimension of the search space grows. The nonlinear SQP optimization method is computationally efficient and has been shown to exhibit superlinear convergernce for convex search spaces [9]. SQP method is therefore well-suited for the problem of UPFC powerflow control setting determination for the proposed cumulative index, which is convex over a wide range of system conditions. Interested readers are referred to the companion paper [22] for

the derivation of the system conditions under which PI_{cum} is guaranteed to be convex. The following sections describe the SQP algorithm and its application to power systems more fully. In general terms, the optimization problem to be solved is:

$$\begin{aligned} \text{Minimize} \quad & f(x) \\ \text{Subject to} \quad & g_i(x) = 0 \quad i = 1, \ldots, m \\ & h_i(x) \leq 0 \quad i = 1, \ldots, q \end{aligned}$$

The usual approach to solving this optimization problem is to use Lagrangian multipliers and minimize the hybrid system:

$$L(x, \lambda) = f(x) - \lambda_i g_i(x) \; i = 1, \ldots, m \tag{11}$$

A. The SQP Algorithm

The SQP approach solves this system of nonlinear equations by applying a (quasi-) Newton method:

$$\text{Min} \;\; 0.5 p^T \bigtriangledown^2 L(x_k, \lambda_k) p + \bigtriangledown L(x_k, \lambda_k)\, p + L(x_k, \lambda_k) \tag{12}$$

$$\begin{aligned} \text{Subject to } \nabla g_i(x_k)^T p + g_i(x_k) &= 0 && (13) \\ \frac{\partial}{\partial x_1} L(x_k, \lambda_k) &= 0 && (14) \\ &\vdots \\ \frac{\partial}{\partial x_n} L(x_k, \lambda_k) &= 0 \\ \frac{\partial}{\partial \lambda_1} L(x_k, \lambda_k) &= 0 && (15) \\ &\vdots \\ \frac{\partial}{\partial \lambda_n} L(x_k, \lambda_k) &= 0 \end{aligned}$$

Equations (14) are known as the Karush-Kuhn-Tucker (KKT) conditions [25] for the original problem. The subproblem of Eq. (12) is minimized sequentially over a linear approximation of the quadratic constraints at each iteration [25], [26] by solving the KKT conditions. Therefore,

given an iterate (x_k, λ_k), the solution of the first order KKT conditions determines the update (x_{k+1}, λ_{k+1}).

In this manner, the minimization process drives the solution toward a desirable KKT solution. The algorithm described is called the Rudimentary SQP (RSQP). The quadratic subproblem is solved to obtain the solution of Eq. (12) along with the Lagrangian multipliers. The iterations stop if p = 0 and x_k satisfies the KKT conditions, otherwise x_k is incremented for the next iteration as x_k=x_{k+1}. A necessary condition for existence of a solution is that the Hessian of the objective function must be positive definite [25].

B. Quasi-Newton Approximation

The disadvantage of the RSQP method is that it requires second order derivatives $\bigtriangledown^2$ L(x_k) to be calculated at each iteration. To overcome this drawback, a quasi-Newton positive definite approximation can be implemented, such that $\bigtriangledown^2$ L(x_k) is replaced by B_k. This B_k is updated using the Broyden-Fletcher-Goldfarb-Shanno (BFGS) [25] method:

$$B_{k+1} = B_k + \frac{q_k q_k^t}{q_k^t P_k} - \frac{B_k P_k P_k^t B_k}{P_k^t B_k P_k} \tag{16}$$

where $P_k = x_{k+1} - x_k$

and $q_k = \bigtriangledown L'(x_{k+1}) - \bigtriangledown L'(x_k)$

where $\bigtriangledown L'(x) = \bigtriangledown f(x) + \sum_{i=1}^{l} \lambda_{(k+1)i} \bigtriangledown g_i(x)$

C. Merit Function Sequential Quadratic Programming

For RSQP, global convergence is guaranteed only when the algorithm is initialized close to a desirable solution, whereas in practice this condition is usually difficult to realize. To remedy this situation and to ensure global convergence, a merit function can be employed, yielding Merit Function Sequential Quadratic Programming (MSQP). This function is, along with the objective function, minimized at the solution of the problem. It serves as a descent function, guiding iterates and providing a measure of progress. The popular absolute value merit function that can be utilized for minimization of *f(x)* is given by:

$$FE(x) = f(x) + \mu\big[\sum_{i=1}^{m} max\{0, h_i(x)\} + \sum_{i=1}^{l} \mid g_i(x) \mid \big] \tag{17}$$

where $h_i(x)$ is an inequality constraint (if it exists). In this paper, the term SQP refers to the merit function based SQP algorithm. This has been implemented in MATLAB [26] for finding the optimal UPFC settings.

V. Simulation Results

Simulations are performed on the IEEE 39 bus test system [7] and the IEEE 118 bus system (Fig. 7) in MATLAB 7.0 on a Pentium IV processor with a CPU speed of 2.4 GHz. The SQP algorithm has been implemented to find the optimal settings of one or more UPFCs over the set of system contingencies. The best placement(s) is one in which there are no line overloads for any line outage and a minimum PI_{cum} is produced.

A. Line Outage 4–5 (IEEE 39 bus system)

For comparison with the LP method [7], the outage of line 4–5 is chosen as the study case. Table I shows the percentage overloaded power (OLP) for the IEEE 39 bus system in the event of outage 4–5, where the OLP is defined by:

$$OLP = \Big(\frac{S_{ij} - S_{ij}^{max}}{S_{ij}^{max}}\Big) \cdot 100\% \tag{18}$$

The outage 4–5 causes overloads to occur on lines 10–13 and 13–14 with OLP being 3.2% and 4.0% respectively. In order to mitigate these overloads, a single UPFC with a powerflow control setting range of $\pm$ 20% of S_{ij}^{max} is used. An exhaustive search was conducted by placing the UPFC on each line in the system and calculating the resulting PI_{cum}. Table II shows the first five top placements for the line outage 4–5 that mitigate all line overloads, the value of PI_{cum}, and powerflows on lines 10–13 and 13–14.

B. Comparison of LP and SQP Nonlinear Optimization

This section compares the LP results reported in [7] with the SQP nonlinear optimization proposed in this paper. The performance of the two methods are compared and analyzed for the same line outage 4–5 and UPFC placements on lines 16–17, 15–16, and 4–14. These particular placements were chosen for study because they are the same placements given in [7], so that a direct comparison between the two methods can be conducted.

TABLE I
CONTINGENCY ANALYSIS RESULTS WITHOUT UPFC

outage	Total OLP	OLP on 10–13	OLP on 13–14
4–5	7.2%	3.2%	4.0%

TABLE II
BEST PLACEMENTS FOR MITIGATING THE OVERLOADS CAUSED BY 4–5

Placement	PI_{cum}	10–13		13–14	
		S_{ij}	S_{ij}^{max}	S_{ij}	S_{ij}^{max}
13 - 14	9.31	438.07	550	448.13	550
10 - 13	10.70	345.18	550	493.66	550
1 - 2	11.16	456.36	550	449.92	550
2 - 3	11.54	519.96	550	520.97	550
4 - 14	12.73	530.46	550	526	550

1) Case I: UPFC on 16–17: Table III shows the resultant optimal powerflow on line 16–17 obtained from the LP and SQP methods. The original flow on the line after the line outage 4–5 without a UPFC is 192.84 MW and -22.31 MVAR. With the UPFC on line 16–17, the SQP settings decrease the powerflow on the line and resolve both overloads. The corresponding UPFC parameters are given in Table IV along with those obtained from the LP method. Both the LP and SQP methods produce powerflow control settings that bring line 10–13 and 13–14 within the maximum line rating. However, the LP method requires that the active power flow through the UPFC reverses direction. From an operational standpoint, it is typically not desirable to change the direction of the powerflow on a line. If the direction of the powerflow on a line changes, it is challenging for the independent system operators (ISO) to dispatch generation and load due to financial transmission rights and other economic constraints. Note also from Table IV, that the LP scheduled powerflows require a much larger injected series voltage and resulting series and shunt powers requiring a much higher rated (and more expensive) UPFC.

TABLE III
COMPARISON OF SQP AND LP POWERFLOW CONTROL FOR PLACEMENT 16–17

	16-17		10-13	13-14
	P_{ij}	Q_{ij}	S_{ij}	S_{ij}
SQP	155.52	60.64	547.78	544.82
LP	-12.63	28.46	528.03	532.53

2) Case II: UPFC on 15–16: Tables V and VI show the results of a UPFC on line 15–16 with SQP and LP control settings. In [7], the authors report that the LP method failed to mitigate overloads for a series voltage injection smaller than 0.35 p.u. This is a very large series injected voltage magnitude. The SQP method provides control settings that result in a much smaller series injected voltage magnitude and lower scheduled shunt and series powerflows.

TABLE IV
COMPARISON OF SQP AND LP CONTROL PARAMETERS FOR PLACEMENT 16–17

	V_{sh}	V_{se}	δ_{sh}	δ_{se}	S_{sh}	S_{se}
SQP	1.00	0.05	-14.9^o	-153.6^o	70.10	8.86
LP	0.90	0.19	-12.9^o	80.2^o	148.80	5.78

TABLE V
COMPARISON OF SQP AND LP POWERFLOW CONTROL FOR PLACEMENT 15–16

	15-16		10-13	13-14
	P_{ij}	Q_{ij}	S_{ij}	S_{ij}
SQP	-266.35	-81.72	545.21	542.19
LP	-424.97	2.20	518.73	528.56

3) Case III: UPFC on 4–14: A UPFC placed on line 4–14 produced better results than UPFC placements on lines 16–17 or 15–16 as it yielded a larger security margin 19.46 p.u and 24 p.u over the lines 10–13 and 13–14, respectively. Once again, SQP outperformed the LP method for the given placement.

TABLE VI
COMPARISON OF SQP AND LP CONTROL PARAMETERS FOR PLACEMENT 15–16

	V_{sh}	V_{se}	δ_{sh}	δ_{se}	S_{sh}	S_{se}
SQP	0.99	0.19	-16.2^o	60.4^o	76.98	89.58
LP	0.88	0.35	-12.9^o	63.5^o	235.60	152.40

TABLE VII
COMPARISON OF SQP AND LP POWERFLOW CONTROL FOR PLACEMENT 4–14

	4-14		10-13	13-14
	P_{ij}	Q_{ij}	S_{ij}	S_{ij}
SQP	-315.31	-83.05	530.46	526.00
LP	-350.36	126.12	532.28	548.20

TABLE VIII
COMPARISON OF SQP AND LP CONTROL PARAMETERS FOR PLACEMENT 4–14

	V_{sh}	V_{se}	δ_{sh}	δ_{se}	S_{sh}	S_{se}
SQP	0.983	0.10	-22.9^o	39.4^o	60.02	35.63
LP	0.991	0.14	-21.2^o	131.8^o	84.10	50.90

Cases I through III clearly show that the SQP algorithm provides better powerflow control settings for a UPFC than the LP algorithm. Additionally, SQP identified placement 4–14 as the best placement, whereas in [7], placement 16–17 was selected as the best placement. In all placements, however, the SQP method provided UPFC powerflow control settings that mitigated the overloaded lines and did so with the potential of a lower rated UPFC.

C. Mitigating Cascading Failures in the IEEE 118 bus system

For the IEEE 118 bus power system (shown in Fig. 7), fourteen cascading blackout scenarios are possible [27] in which, each of these cascading blackouts is initiated by a single line contingency, and the successive removal of the next most heavily overloaded line in the system until the system collapses. The SQP method is used in this example to provide UPFC powerflow settings for three different scenarios to mitigate the cascade.

1) Scenario I - line outage 4–5: The removal of line 4–5 overloads line 5–11 by 15.85% as shown in Table IX. The subsequent removal of this line causes overloads in lines 5–6, 6–7 and 7–12. The loss of any of these lines leaves the surrounding lines with insufficient capacity to accommodate the power flowing away from the generator at bus 10. In order to prevent this cascading outage, it is necessary to mitigate the initial overload caused by the outage of line 5–11. The solution provided by evolutionary algorithm for placement and the SQP method for

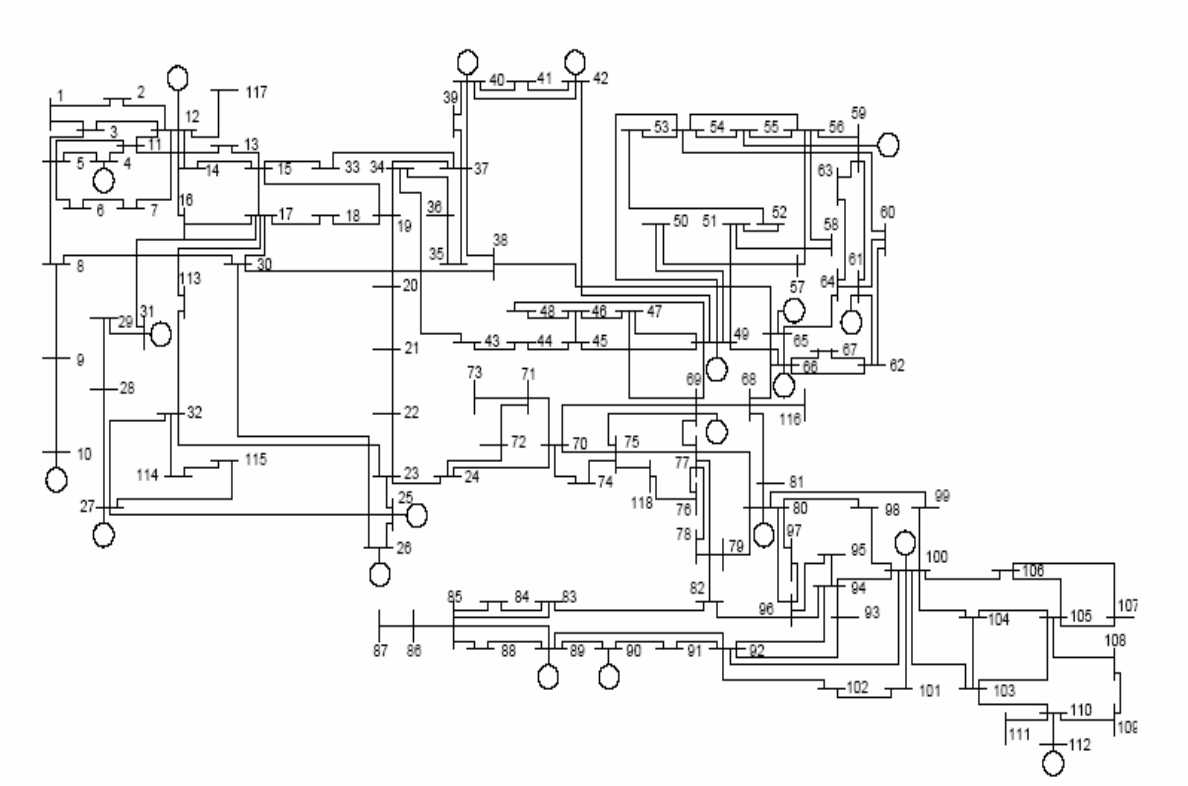

Fig. 7. One line diagram of the IEEE 118 bus system

the long term control settings is to place two UPFCs on lines 5–11 and 7–12 with the power flow set points given in Table IX. This solution reduces the number of initial overloads to zero and averts the cascading failure. The CPU time required for finding the optimal solution is 0.461 sec.

TABLE IX
SCENARIO 4–5

	NOL	OLP	5-11		Voltage
			S_{ij}	S_{ij}^{max}	at bus 5
Without UPFC	1	15.85	134.27	115.89	0.99
With UPFCs	0	0	101.90	115.89	1.00

Placement	w/o Control		w Control	
	P_{ij}	Q_{ij}	P_{ij}	Q_{ij}
5 - 11	131.79	-25.65	101.85	3.32
7 - 12	42.66	-37.25	29.69	-9.36

TABLE X
SCENARIO 37–39

	NOL	OLP	37-40		Voltage
			S_{ij}	S_{ij}^{max}	at 37
Without UPFC	1	24.18	82.33	66.29	0.9723
With UPFCs	0	0	54.99	66.29	0.9696

Placement	w/o Control		w Control	
	P_{ij}	Q_{ij}	P_{ij}	Q_{ij}
37 - 40	79.60	-20.99	54.98	-0.71
49 - 51	66.05	26.46	60.08	26.76

2) Scenario II - line outage 37–39: The outage of line 37–39 overloads the line 37–40 and the re-directed power through the transformer 37–38 makes the device vulnerable. This transformer can be protected by installing two UPFCs on lines 37–40 and 49–51 with powerflow control settings as shown in Table X. The voltage at bus 37 is maintained at its steady state value by decreasing the reactive power injection at the bus from -20.99 p.u. to -0.71 p.u. while the reactive injection at the other UPFC remains approximately the same. The required CPU time to find the powerflow control settings for these two devices is 0.511 sec.

3) Scenario III - line outage 89–92: Buses 89 and 92 are connected by parallel lines. One of these lines is a high impedance line (circuit1) and the other is of low impedance (circuit2).

TABLE XI
SCENARIO 89–92

	NOL	OLP	82-83		91-92	
			S_{ij}	S_{ij}^{max}	S_{ij}	S_{ij}^{max}
Without UPFC	2	28.374	97.42	81.92	46.1	42.12
With UPFCs	0	0	73.20	81.92	8.04	42.12
Placement			w/o Control		w Control	
			P_{ij}	Q_{ij}	P_{ij}	Q_{ij}
82–83			-85.14	47.16	-62.33	37.34
91–92			45.242	-8.87	0.12	6.59

Removal of either of these lines causes overloads on line 82–83 with an OLP 18.92% and on line 91–92 with an OLP 9.45%. Placing UPFCs on lines 82–83 and 91–92 with the control settings given in Table XI mitigates the cascading failure that might occur by tripping either of the double lines. The CPU time for this scenario was 0.613 sec.

VI. Conclusions

The UPFC is a fast acting device which can effectively control and improve power flows in the modern power system. For the long term control of this device, a fast, robust and reliable SQP based method has been proposed and implemented in this paper. A comparison of the SQP method with LP optimization indicates that the powerflow control settings given by SQP are more reliable as the SQP results yield higher security margins for the power flows on the lines and voltages at the buses. The control setting coordination among multiple UPFCs does not pose a problem during the optimization process for convex search spaces. SQP was shown to provide control settings in both small and large test systems with computational efficiency.

Acknowledgements

The authors gratefully acknowledge the assistance provided by Drs. W. Shao and V. Vittal in providing assistance with the system data and results for the LP method in this paper. The authors gratefully acknowledge the support of the National Science Foundation under grant

CNS-0420869 and the DOE Energy Storage Program through Sandia National Laboratories under BD-0071-D.

REFERENCES

[1] V. Azbe, U. Gabrijel, D. Povh, and R. Mihalic, "The energy function of a general multimachine system with a unified power flow controller," in *IEEE Transactions on Power Systems*, vol. 20, 2005, pp. 1478–1485.

[2] S. N. Singh, K. S. Verma, and H. O. Gupta, "Optimal power flow control in open power market using unified power flow controller," in *Power Engineering Society Summer Meeting*, vol. 3, Jul 2001, pp. 1698–1703.

[3] H. C. Leung and T. S. Chung, "Optimal power flow with a versatile FACTS controller by genetic algorithm," in *IEEE Power Engineering Society Winter Meeting*, vol. 4, Jan 2000, pp. 2806–2811.

[4] P. Bhasaputra and W. Ongsakul, "Optimal power flow with multi-type of FACTS devices by hybrid TS/SA approach," in *IEEE International Conference on Industrial Technology*, vol. 1, Dec 2002, pp. 285–290.

[5] H. A. Abdelsalam, G. A. M. Aly, M. Abdelkrim, and K. M. Shebl, "Optimal location of the unified power flow controller in electrical power systems," in *IEEE PES Power Systems Conference and Exposition*, vol. 3, Oct 2004, pp. 1391–1396.

[6] A. Armbruster, M. Gosnell, B. McMillin, and M. L. Crow, "The maximum flow algorithm applied to the placement and distributed steady-state control of UPFCs," in *Proceedings of the 37th Annual North American Power Symposium*, 2005, pp. 77–83.

[7] W. Shao and V. Vittal, "LP-based OPF for corrective FACTS control to relieve overloads and voltage violations," *IEEE Transactions on Power Systems*, vol. 21, no. 4, pp. 1832–1839, 2006.

[8] A. E. Eiben and J. E. Smith, *Introduction to Evolutionary Computing*. Springer, 2003.

[9] L. T. Biegler, T. F. Coleman, A. R. Conn, and F. N. Santosa, *Large-Scale Optimization with Applications - Part II: Optimal Design and Control*. Springer-Verlag Inc, 1997.

[10] J. Bian, D. G. Ramey, R. J. Nelson, and A. Edris, "A study of equipment sizes and constraints for a unified power flow controller," in *IEEE Transactions on Power Delivery*, vol. 12, 1997, pp. 1385 – 1391.

[11] K. Visakha, D. Thukaram, L. Jenkins, and H. P. Khincha, "Selection of UPFC suitable locations for system security improvement under normal and network contingencies," in *Conference on Convergent Technologies for Asia-Pacific Region*.

[12] J. Momoh and A. U. Chuku, "Application of expert system for improved contingency analysis and optimal correction," in *Proceedings of the Twenty-First Annual North-American Power Symposium*, vol. 15, Oct 1989, pp. 33 – 37.

[13] T. S. Sindhu and L. Cui, "Contingency screening for steady state security analysis by using FFT and ANNs," in *IEEE Transactions on Power Systems*, vol. 15, 2000, pp. 421 – 426.

[14] A. Mohamed and G. B. Jasmon, "Voltage contingency selection technique for security assessment," in *IEE Proceedings-Generation, Transmission and Distribution*, vol. 136, 1989, pp. 24 – 28.

[15] I. Musirin and T. K. A. Rahman, "On-line voltage stability based contingency ranking using fast voltage stability index (FVSI)," in *IEEE/PES Asia Pacific Transmission and Distribution Conference and Exhibition*, vol. 2, 2002, pp. 1118 – 1123.

[16] I. Musirin, T. Khawa, and A. Rahman, "Simulation technique for voltage collapse prediction in power system," in *Student Conference on Research and Development*, 2002.

[17] J. Zhang, Y. F. Guo, and M. H. Yang, "Assessment of voltage stability for real-time operation," in *IEEE Power India Conference*, 2006, pp. 5–10.

[18] P. Kessel and H. Glavitsch, "Estimating the voltage stability of a power system," in *IEEE, Transactions on Power Delivery*, vol. PWRD-1, 1986.

[19] B. Gao, G. K. Morison, and P. Kundur, "Voltage stability evaluation using modal analysis," in *IEEE Transactions on Power Systems*, vol. 7, 1992.

[20] M. Moghavvemi and F. M. Omar, "Technique for contingency monitoring and voltage collapse prediction," in *IEEE Proceeding on Generation, Transmission and Ddistribution*, vol. 145, 1998, pp. 634–640.

[21] G. B. Jasmon and L. H. C. Lee, "New contingency ranking technique incorporating a voltage stability," in *IEE Proceedings-Transmission and Distribution*, 1993, pp. 87 – 90.

[22] R. P. Kalyani, M. L. Crow, and D. R. Tauritz, "A nonlinear optimization approach for UPFC power flow control and voltage security: Sufficient system constraints for optimality," *IEEE Transactions on Power Systems*, 2007, in submission.

[23] C. Reis and F. P. M. Barbosa, "A comparison of voltage stability indices," in *IEEE Mediterranean Electrotechnical Conference*, 2006, pp. 1007 – 1010.

[24] S. Boyd and L. Vandenberghe, *Convex Optimization*, 1st ed. Cambridge University Press, 2004.

[25] M. S. Bazaraa, H. D. Sherali, and C. M. Shetty, *Nonlinear Programming: Theory and Algorithms*, 2nd ed. Wiley Press, 1993.

[26] T. Coleman, M. A. Branch, and A. Grace, *Optimization Toolbox for Use with Matlab*, The Math Works, Inc, 1999.

[27] B. H. Chowdhury and S. Bharave, "Creating cascading failure scenarios in interconnected power systems," in *IEEE Power Engineering Society General Meeting*, June 2006.

PAPER 3

Optimal Placement and Control of Unified Power Flow Control Devices using Evolutionary Computing and Sequential Quadratic Programming

Radha P. Kalyani, Electrical and Computer Engineering Dept

University of Missouri - Rolla

Rolla, Missouri 65409

Email: rpk5f9@umr.edu

Mariesa L. Crow, Dean, School of Materials, Energy Earth Resources

University of Missouri - Rolla

Rolla, Missouri 65409

Email: crow@umr.edu

Daniel R. Tauritz, Computer Science Department

University of Missouri - Rolla

Rolla, Missouri 65409

Email: tauritzd@umr.edu

ABSTRACT

A crucial factor effecting modern power systems today is power flow control. An effective means for controlling and improving power flow is by installing fast reacting devices such as a Unified Power Flow Controller (UPFC). For maximum positive impact of this device on the power grid, it should be installed at an optimal location and

employ an optimal real-time control algorithm. This paper proposes the combination of an Evolutionary Algorithm (EA) to find the optimal location and Sequential Quadratic Programming (SQP) to optimize the UPFC control settings. Simulations are conducted using the classic IEEE 118 bus test system. For comparison purposes, results for the combination of a greedy placement heuristic (H) and the SQP control algorithm are provided as well. The EA+SQP combination is shown to outperform the H+SQP approach.

I. Introduction

With the ever-increasing complexities in power systems across the globe and the growing need to provide stable, secure, controlled, economic, and high-quality electric power-especially in today's deregulated environment - it is envisaged that Flexible AC Transmission System (FACTS) devices are going to play a critical role in power transmission systems [1]. These devices enhance the stability of the power system both with their fast control characteristics and continuous compensating capability. A FACTS device can control power flow and increase the transmission capacity effectively over an existing transmission corridor by placing the device at an optimal location [1].

There are a variety of methods proposed for optimizing the placement of FACTS devices [2]–[7]. The Unified Power Flow Controller (UPFC) is the most powerful, but also the most expensive, device in the family of voltage-source-converter-based FACTS devices, but there are very few papers that suggest a simple and reliable method [5]–[7] for determining the suitable location of UPFCs for enhancing the loadability of the power system over different topologies. The placement of UPFCs is a very complex problem, even under the consideration of steady-state conditions only (neglecting dynamic controls). An optimal UPFC placement must incorporate not only each possible system topology (line outages, load profiles, etc.) but must also consider the entire range of possible control settings which may themselves be dependent on system topology.

UPFC placement is a very complex optimization problem for three reasons:

1) Evaluating the quality of a placement is a computationally intensive task.
2) The search space grows combinatorially with the size of the power system and the number of UPFC devices.

3) Non-linear dependencies between the placement of individual UPFC devices result in a search space with many local optima.

The first two reasons combined make exhaustive search infeasible, while the third reason defeats traditional search algorithms. Evolutionary Algorithms (EAs) are appropriate in this case as they are well-suited to finding near optimal solutions in a reasonable amount of time for very large, non-smooth, discontinuous, non-differentiable objective functions. Additionally, the Sequential Quadratic Programming (SQP) [8] has been shown to be an effective approach to determining the optimal power flow control setting for the UPFC [9], [10].

This paper proposes employing the combination of EA and SQP (EA+SQP) for the placement and control setting, respectively, of UPFC devices. The organization of this paper is as follows: Section II defines the problem that must be solved using the EA+SQP approach. Section III describes the UPFC model and Section IV briefly describes the UPFC placement EA specifics. Section V describes the results of the simulations conducted using the proposed approach, while Section VI presents the conclusions and ideas for future work.

II. UPFC Placement and Control

UPFC placement in a bulk power system is a crucial problem as it significantly impacts active power flow. To date, several authors [2], [3] have proposed the placement of this device from an economic perspective, i.e., to reduce the production cost or the installation cost of the device. Other placement algorithms consider only a fixed topology system while determining the power flow control setting necessary for the placement, such that the UPFC placement is suited only to a particular load and generation profile. But in reality, the placement and control algorithm of the UPFC should be able to accommodate any contingency or disturbance.

UPFCs, by virtue of their fast controllability, are expected to maintain the stability and security margin of highly stressed power systems. The proposed EA+SQP combination of algorithms provides an approach for placing and determining the steady-state power flow control settings of UPFCs for any contingency in the system.

There are several indices/methods [4], [5] proposed in literature to evaluate the quality of a specific placement of FACTS devices. In this paper, a Performance Index (PI)(1), is used as a metric to determine the optimality of the placement and control setting of the UPFC. PI index

minimizes line overloads as higher overloads incur heavier penalties than lower overloads and minimizes power flow imbalances resulting in a more even utilization of all lines in the system.

$$PI = \sum_{SLC} \sum_{all\ Lines} \left(\frac{S_i}{S_i^{max}} \right)^2 \tag{1}$$

where S_i is the apparent power flow on line i for each Single Line Contingency (SLC) and S_i^{max} is the rating of the line i.

Fig. 1 shows the PI metric space (interpolation of 21 equidistant control setting samples) for a random contingency on the line between buses 23-32 in the IEEE 118 bus test system [11] with a single UPFC device placed on the randomly selected line 26-30. The allowable power flow control settings for the UPFC are in the range of $\pm$ 20 % of the maximum power flow (P_{max}) value of the line. The PI space for the two randomly selected UPFC placements

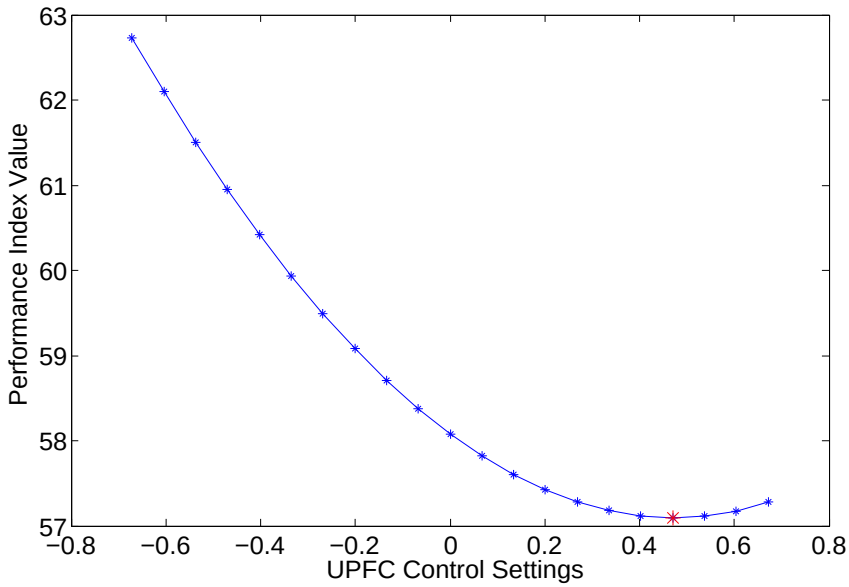

Fig. 1. PI curvature for single UPFC placement 26-30 and SLC 23-32

5-8 and 26-30 over a sampling of control settings for a single randomly selected SLC 23-32 is shown in Fig. 2. The vertical line in this figure indicates the best UPFC power flow control settings found by SQP. The shape of the control space suggests the absence of local minima.

Based on this result, the constrained gradient descent technique SQP [8] was chosen as control algorithm since the gradient descent technique is computationally efficient in the absence of multiple minima. While the results suggest that the PI metric results in a convex surface, further analysis is required to prove that the surface is convex under all operating conditions and placements.

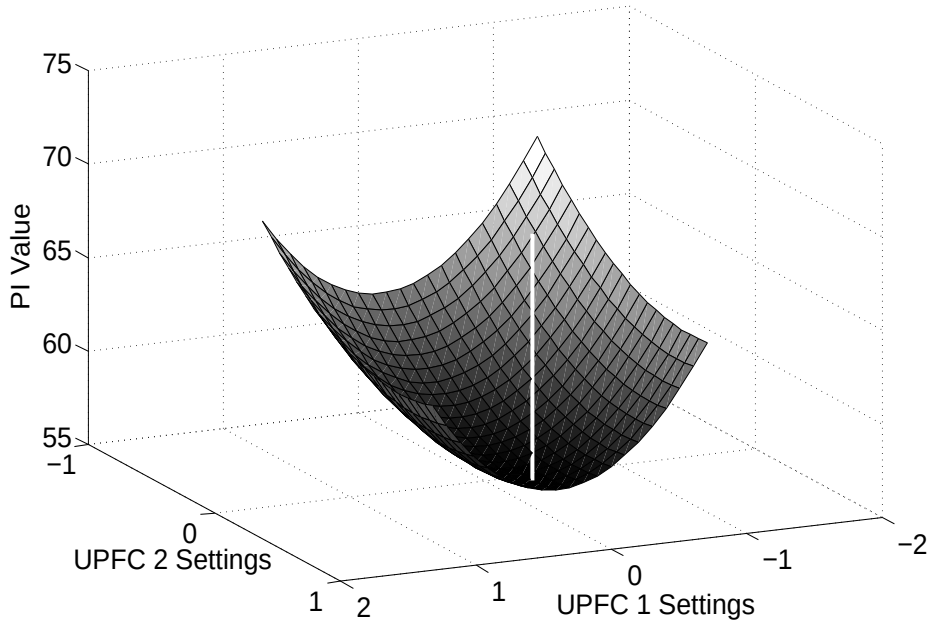

Fig. 2. PI surface for two UPFC placements 5-8, 26-30 and SLC 23-32

III. UPFC Model

The function of the UPFC in the network is to control the active power flow through a line to a specified value. By controlling the active power through a specified line, the remaining lines in the system adjust their power flow according to the physics of the system. The lossless steady state model of UPFC [12] delivers active power to one of the buses of $Line_{ij}$ and draws a corresponding amount of active power from the other bus of the same line, shown in Fig. 3. It is assumed that the installation of the UPFC may increase or decrease the active power flow through $Line_{ij}$ by no more than 20% of the line capacity P_{max}.

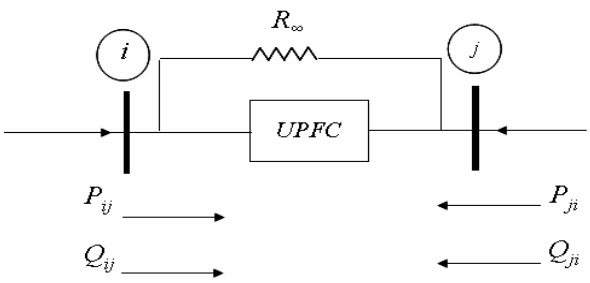

Fig. 3. UPFC injection model

IV. UPFC PLACEMENT EA

EAs are robust search and optimization algorithms based on natural selection in environments and natural genetics in biology [13]. Table I shows the specifications of the EA.

A. Fitness Function

The objective of this optimization problem is to minimize the overloading of the system over all SLCs by optimizing the placement of multiple UPFC devices. In terms of the PI metric (1), this is formulated as a minimization problem. As fitness per definition should be maximized, the fitness function in this case is equal to the negative of the PI metric.

TABLE I
SPECIFICATIONS OF EA FOR PLACEMENT OF UPFC

Representation	Fixed size vector of integers
Initialization	70% random, 30% seeded
Parent Selection	Tournament Selection
Recombination	Uniform Crossover
Mutation	Customized
Survivor Selection	Elitist Deterministic Rank Based Steady State
Termination	Fixed Number of Generations

B. Representation

Each individual in a typical EA consists of a set of genes which encode a trial solution to the problem to be solved (i.e., the environment). Here a trial solution consists of a set of

UPFC placements, expressed as positive integers, each of which indicates a line in the IEEE 118 bus test system where a UPFC device should be placed. The number of integers (genes) in each individual is fixed to N_{UPFC}, the number of UPFCs to be installed in the IEEE 118 bus power system for decreasing the loadability of the system. For example, for a placement with $N_{UPFC} = 4$, a single individual in the population might be as shown in Fig. 4.

10	27	50	117

Fig. 4. Example UPFC placement individual

C. Initialization

The number of individuals in the population is specified by the parameter μ. The population consists for 70% of randomly initialized individuals, the remaining 30% are seeded from previous runs and heuristics.

D. Parent Selection & Recombination

A mating pool is generated by conducting a tournament among $TournSize$ individuals randomly selected from the population. During each tournament, the two fittest individuals are selected and placed into the mating pool. This process continues until the mating pool is filled, i.e., *NParents* are generated.

The number of offspring that can be generated by recombination is specified by the parameter λ. The parents for the recombination are randomly selected from the mating pool and the offspring are generated depending on the recombination parameter Cross Over Rate (*CORate*). If a random number generated is less than the *CORate*, then two offspring are generated by implementing uniform crossover; otherwise the parents are cloned.

E. Mutation

Each offspring generated by recombination is mutated depending on a mutation probability *MutationRate*. Mutation here reflects the movement of the UPFC to its neighboring lines. This

movement acts as neighborhood (local) search for each placement to find better individual. A gene in a placement will be mutated to its neighbor. A line is a neighbor to another line if it has a common bus. Therefore when a UPFC is chosen for mutation depending on *MutationRate*, it is moved from the present line to its neighboring lines. This acts as a local search for finding a better placement in the neighborhood of existing placement [6]. Figures 5 and 6 show a small network with lines 49-53, 53-55, 55-56, 55-58, 55-54 and 54-53 connected to each other.

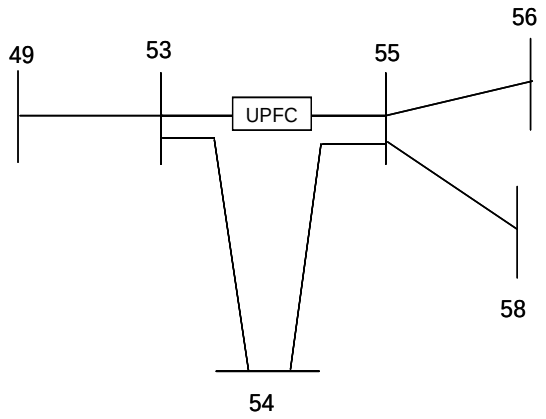

Fig. 5. UPFC initially placed on line 53-55

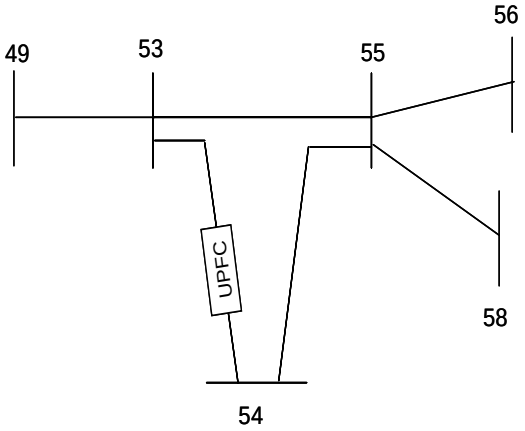

Fig. 6. UPFC moved to the neighboring line 53-54 as a result of mutation

Each of these lines are prone to mutation since the UPFC is initially installed on line 53-55. It shares a common bus with all of the remaining lines. Through the mutation operation mentioned above, the UPFC may be moved from line 53-55 to the neighboring line 53-54.

F. Reproduction Correction

Reproduction correction is an extra stage in the EA to check if any of the line numbers are duplicated in the placement, which is an invalid condition in an actual power system. Fig. 7(a) shows invalid placement and Fig. 7(b) shows its corresponding corrected placement. In this placement, two UPFC devices are placed on the same line 50 (30-38). This can be corrected by checking the placement after the offspring are generated and moving the device to lines away from the present installation 50 randomly. By implementing validation, every placement is ensured to be unique before it is evaluated for its PI value.

10	50	50	117

(a) Invalid Placement

10	50	172	117

(b) Corrected Placement

Fig. 7. Example invalid and valid placements

G. Survivor Selection

A steady state EA with rank based elitist is used for survival selection. Steady state refers to the $(\mu+\lambda)$ strategy where $\mu \gg \lambda$. An elitist is used in an attempt to prevent the loss of current fittest member of the population. λ offspring are created and exact same number of least fit individuals are removed from population of $(\mu+\lambda)$ by means of rank based selection. In a rank based selection the total population is sorted according to fitness, and the best μ individuals are selected to survive for the next generation. This deterministic approach is chosen over stochastic approach for faster convergence, as the given fitness function is computationally intensive.

H. Termination Condition

While the theoretical lower bound on the PI metric (1) is zero, the actual minimal value in any given scenario is unknown and cannot therefore be used as a stopping criterion. A more

practical issue is the high computational cost of computing the PI metric. To put reasonable bounds on the duration of the experiments, a fixed number of generations is used as the termination condition.

V. Simulation Results

Simulations are conducted on the IEEE 118 bus test system [11] for evaluating the proposed EA+SQP approach. This dataset has 118 buses, 186 lines and 20 generators. Individuals in the EA population encode trial solutions in the form of UPFC placements. The fitness of an individual is computed by having SQP optimize the PI metric (1). The speed and quality of convergence of the EA depends on various EA strategy parameters. In this paper three parameter sets (Table II) are compared in determining the best placement for two to five UPFCs. Each parameter set is run for 100 generations (termination condition based on practical time limitations) and repeated for five runs in order to be able to perform a statistical analysis on the comparison of the difference of two means.

TABLE II
EA Parameter sets

Parameter set	μ	$TournSize$	λ	NParents	CO Rate	Mutation Rate
PSet1	150	15	10	15	0.7	0.1
PSet2	100	8	10	15	0.7	0.2
PSet3	50	3	5	15	0.9	0.5

Table III shows the mean and standard deviation of highest fitness (*HFit*) over five runs for three parameter sets and different UPFC placements. These sets are further tested for different means by using the Wilcoxon Rank Sum Test (WRST) for two to five placements. WRST performs a two-sided rank sum test of the hypothesis on two independent samples coming from distributions with equal means, and returns the probability value (P) and null hypothesis (NH) [14] from the test.

For instance, WRST is conducted on every combination of the three parameter sets for two UPFCS as shown in Table IV. The output of the hypothesis and the P-values are as shown in the same table. Based on the hypothesis and mean of *HFit*, parameter set 1 (PSet1) is determined

as the one which gives the best promising placement for two UPFCs. This placement is on lines 69 (42-49) and 158 (92-94). Performing similar statistical analysis with the parameter sets shown in Table II, it is determined that PSet1, PSet2 and PSet1 yield best placements for three, four and five UPFCs, respectively. A greedy placement Heuristic(H) [7] in conjunction with

TABLE III
MEAN AND STANDARD DEVIATION OF $HFit$ OVER FIVE RUNS

Number of UPFCs	Parameter Set	Mean	Standard Deviation
2	PSet1	-50.6412	0.0894
	Pset2	-50.7295	0.1002
	Pset3	-51.0494	0.2127
3	Pset1	-49.4862	0.0782
	Pset2	-49.6869	0.2037
	Pset3	-49.6997	0.2240
4	Pset1	-48.6331	0.2650
	Pset2	-48.4581	0.1825
	Pset3	-48.7696	0.3052
5	Pset1	-47.4544	0.2513
	Pset2	-48.2087	0.3878
	Pset3	-48.5432	0.4641

SQP (H+SQP) is implemented to compare the results obtained from EA+SQP. This heuristic is a pruned exhaustive search, in which the top fifty best placements found by single UPFC placement search are paired to find the best placement with two UPFCs ($50C_2$ combinations). Similarly for three UPFCs $20C_3$ combinations, for four $10C_4$ combinations and for five $8C_5$ combinations are searched for finding best placement with H+SQP approach.

The number of overloads (NOL) for 118 bus system over all SLCs is 119. The total overloaded power (TOP) is 25.88 p.u and average PI is 56.49 p.u over all SLCs. For finding the best placement of single UPFC, exhaustive search (ES) is conducted with the settings determined by SQP. Table V tabulates N_{UPFC}, NOL, TOP and average PI for placement approaches ES, EA and H while determining the control settings with SQP.

Figures 8 through 10 show the comparison plots of the EA+SQP and H+SQP approaches for 0 to 5 UPFCs. It is evident from the plots that as the number of UPFCs increase, NOL, TOP and average PI decrease considerably, also the EA outperforms the heuristic placement

TABLE IV
EXPERIMENTAL RESULTS OF WRST ON THREE PARAMETER SETS

Parameter Sets Compared	Alpha Value	P Value from WRST	Conclusion
1 - 2	0.05	0.7222	Accept NH
1 - 3	0.05	0.0317	Reject NH
2 - 3	0.05	0.0215	Reject NH

approach. Another advantage of the EA over ES and H is that it is faster, as it executes a loadflow fewer times than the heuristic. For example, the number of loadflow calls for the heuristic (H+SQP) with two UPFCs are $50C_2 \cdot 186 = 227850$ whereas for the EA (for PSet1) it is $(150 + 10 \cdot 100) \cdot 186 = 213900$ calls. With ES the number of loadflow calls will be larger since $186C_2$ combinations have to be run to find the optimal placement. Also as the number of devices increase the heuristic becomes less precise due to restriction on number of combinations that can be searched for finding optimal placement. But for EA, varying selective pressure for the same population size might yield better solutions (placements).

TABLE V
COMPARISON OF ES, EA AND H

Approach	N_{UPFC}	Placement	NOL	TOP	Average PI
ES	1	42-49	119	25.711	52.222
EA	2	42-49, 100-106	113	25.097	50.661
H	2	42-49, 82-83	117	25.5	50.6813
EA	3	42-49, 47-69, 100-106	112	24.921	49.112
H	3	42-49, 68-69, 82-83	116	25.362	49.553
EA	4	42-49, 47-69, 68-69, 100-106	107	24.748	48.218
H	4	42-49, 68-69, 82-83, 103-110	115	25.267	48.4661
EA	5	3-5, 42-49, 47-69, 68-69, 100-106	107	24.661	46.752
H	5	3-5, 42-49, 68-69, 83-85, 92-94	114	25.154	46.829

VI. CONCLUSION

This paper proposed and implemented an EA+SQP approach for the placement of UPFCs in a power network. It can be concluded from the results that the loadability of the system

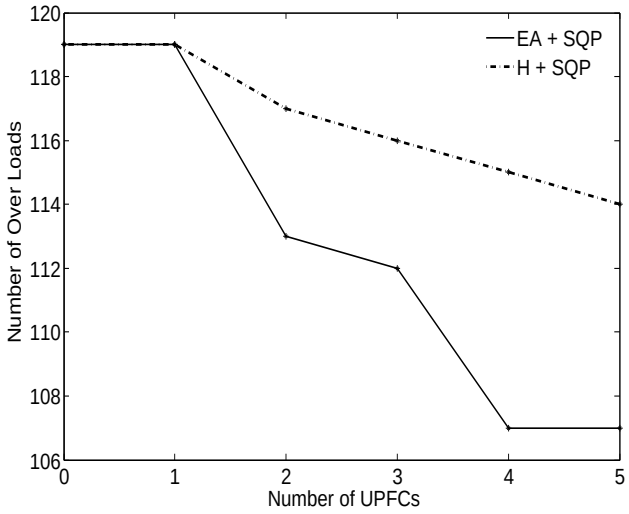

Fig. 8. Comparison of EA and H for NOL

increased and better power flow control (during SLCs) was achieved by choosing the optimal placement and control algorithm for UPFCs. Comparison of the EA+SQP and H+SQP approaches demonstrated that robust algorithms such as EAs could find the optimal/near optimal solution for the placement problem at minimum time expense. Also, EA+SQP outperforms pruned exhaustive search H+SQP. Further studies need to be performed on optimizing the EA strategy parameters as well as employing more sophisticated EAs such as memetic EAs. Another future task is to analyze the placement of the devices from a stability perspective.

ACKNOWLEDGMENTS

This work was supported in part by the National Science Foundation under grant CNS-0420869.

REFERENCES

[1] G. H. Narain and G. Laszlo, *Understanding FACTS: Concepts and Technology of Flexible AC Transmission Systems*. Wiley-IEEE Press, 1999.

[2] H. C. Leung and T. S. Chung, "Optimal power flow with a versatile FACTS controller by genetic algorithm," in *IEEE Power Engineering Society Winter Meeting*, vol. 4, Jan 2000, pp. 2806–2811.

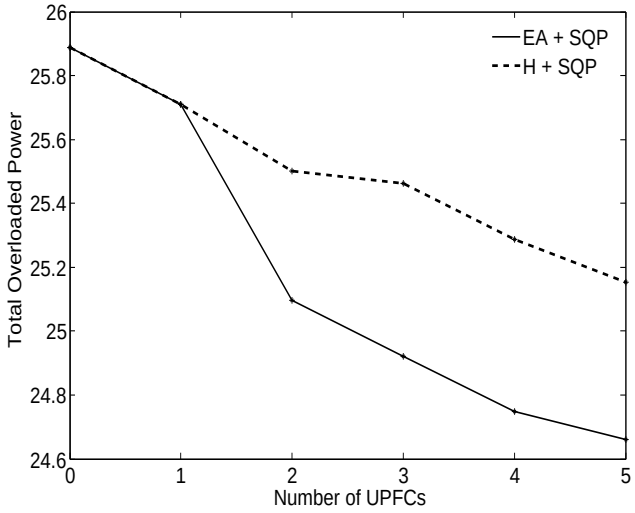

Fig. 9. Comparison of EA and H for TOP

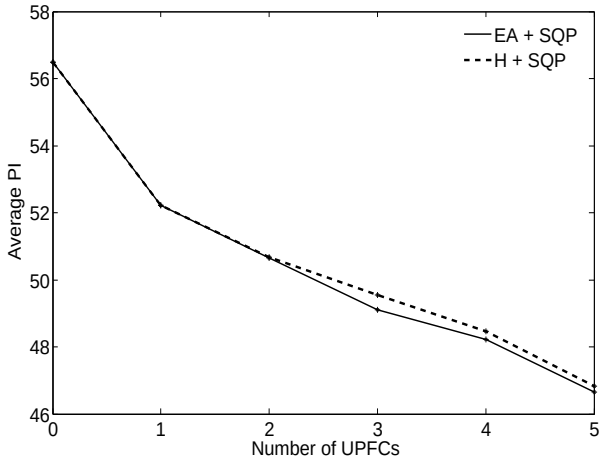

Fig. 10. Comparison of EA and H for average PI

[3] S. N. Singh and A. K. David, "A new approach for placement of FACTS devices in open power markets," *IEEE Power Engineering Review*, vol. 21, no. 9, pp. 58–60, 2001.

[4] S. N. Singh, K. S. Verma, and H. O. Gupta, "Optimal power flow control in open power market using unified power flow controller," in *Power Engineering Society Summer Meeting*, vol. 3, Jul 2001, pp. 1698–1703.

[5] K. Visakha, D. Thukaram, L. Jenkins, and H. P. Khincha, "UPFC suitable locations for system security improvement under normal and network contingencies," in *Conference on Convergent Technologies for Asia-Pacific Region*, vol. 2, Oct 2001, pp. 755–760.

[6] J. Chaloupek, D. R. Tauritz, B. McMillin, and M. L. Crow, "Evolutionary optimization of flexible AC transmission system device placement for increasing power grid reliability," in *6th International Workshop on Frontiers in Evolutionary Algorithms*, 2005.

[7] A. Armbruster, M. Gosnell, B. McMillin, and M. L. Crow, "The maximum flow algorithm applied to the placement and distributed steady-state control of UPFCs," in *Proceedings of the 37th Annual North American Power Symposium*, 2005, pp. 77–83.

[8] T. Coleman, M. A. Branch, and A. Grace, *Optimization Toolbox for Use with Matlab*, The Math Works, Inc, 1999.

[9] W. Siever, R. P. Kalyani, M. L. Crow, and D. R. Tauritz, "UPFC control employing gradient descent search," in *Proceedings of the 37th Annual North American Power Symposium*, Oct 2005, pp. 379–382.

[10] W. B. Siever, D. R. Tauritz, and A. Miller, "Improving grid fault tolerance by optimal control of FACTS devices," in *Proceedings of First International ICSC Symposium on Artificial Intelligence in Energy Systems and Power*, 2006.

[11] R. Christie, "Power systems test case archive: 118 bus power flow test case," May 1993. [Online]. Available: http://www.ee.washington.edu/research/pstca/pf118/pg_tca118bus.htm

[12] V. Azbe, U. Gabrijel, D. Povh, and R. Mihalic, "The energy function of a general multimachine system with a unified power flow controller," in *IEEE Transactions on Power Systems*, vol. 20, 2005, pp. 1478–1485.

[13] A. E. Eiben and J. E. Smith, *Introduction to Evolutionary Computing*. Springer, 2003.

[14] "Statistics Toolbox for use with Matlab," 1999. [Online]. Available: http://www.mathworks.com/products/statistics

SECTION

2. SIMULATION RESULTS

Additional simulation results are presented in this section supporting the individual active and reactive power control (*P* Control and *Q* Control) for the UPFC. Simulations are conducted on IEEE 118 bus system (Figure 2.1) with 186 lines and 20 generators.

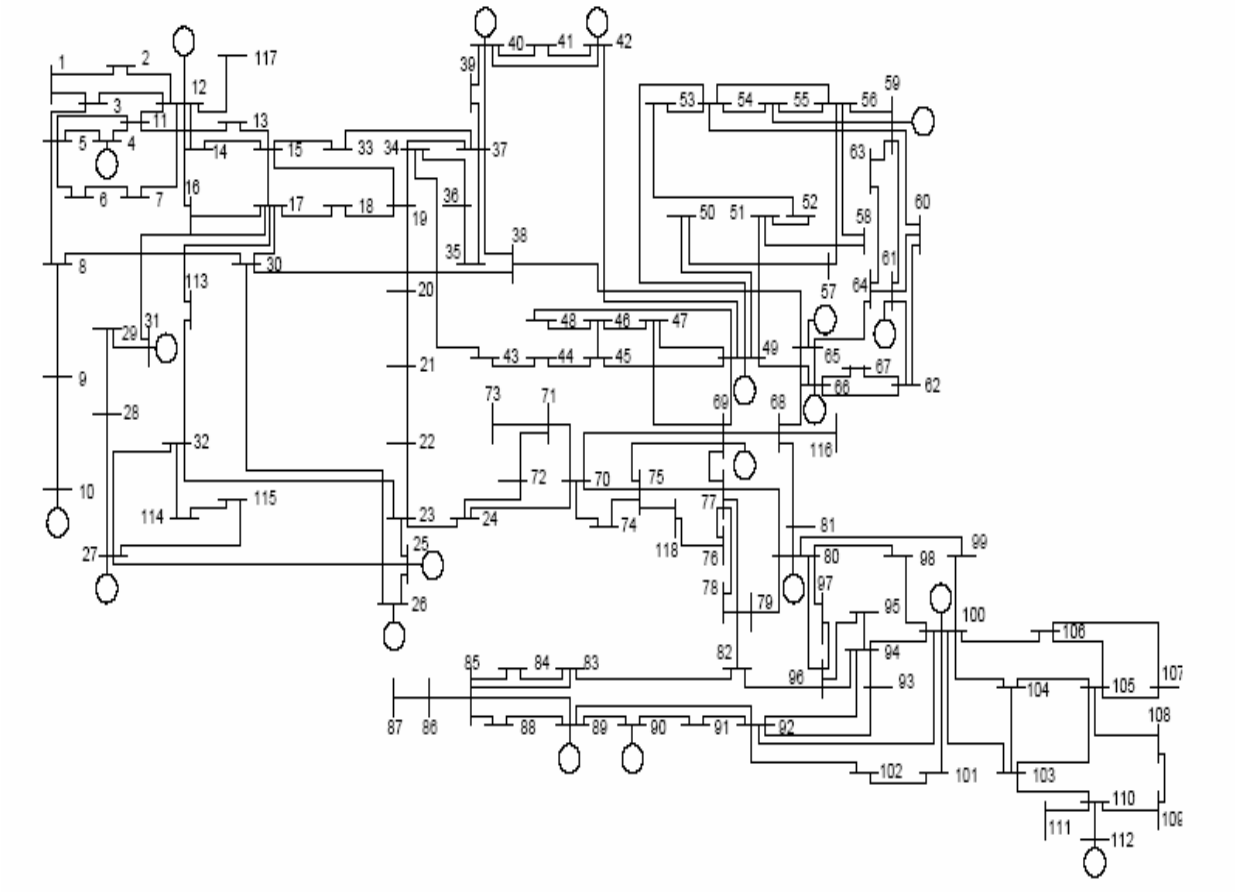

Figure. 2.1 Line diagram of IEEE 118 bus system

2.1. RESULTS FOR *P* CONTROL

This section includes the results of the *P* Control in the 118 bus system for single line contingencies (SLC) and different random UPFC placements in the system.

Figure 2.2 shows the PI_{MVA} metric space (interpolation of 21 equidistant control setting samples) for a random SLC 23-32 in the IEEE 118 bus test system with a single UPFC device placed on the randomly selected line 26-30. Using SQP to minimize PI_{MVA} , it can be observed that as the control setting of the UPFC device varies in the range [1.52 p.u, 2.82 p.u], the PI_{MVA} reaches a minimum value of 56.56 at 2.64 p.u.

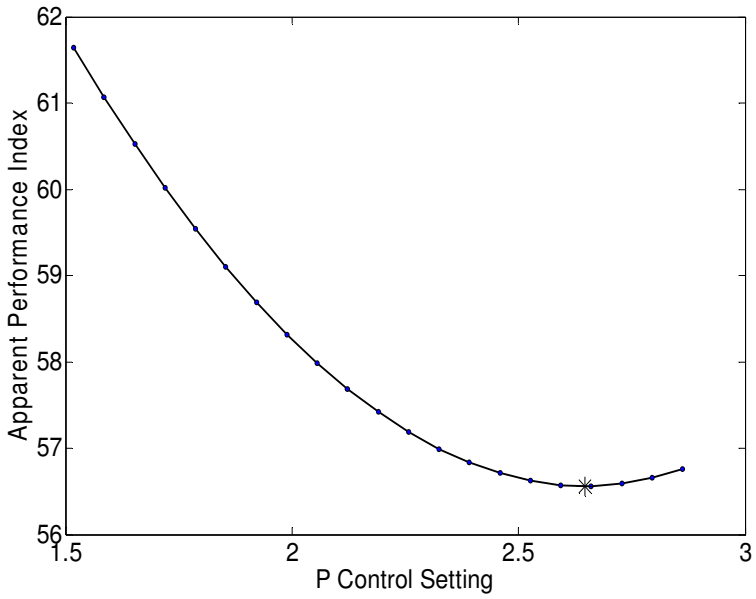

Figure. 2.2 *P* control of the single UPFC placement 26-30 and SLC 23-32

Another UPFC has been installed in the system between buses 5 and 8. Figure 2.3 shows the two-dimensional PI_{MVA} space for the two UPFC placements 5-8 and 26-30 over

a sampling of control settings for the same SLC 23-32. The vertical line in this figure indicates the minimum PI_{MVA} value (55.19) for the best UPFC power flow control settings [-3.331 p.u, 2.384 p.u] of the two UPFCs, respectively (determined by SQP).

2.2. RESULTS FOR *Q* CONTROL

Figures 2.4 and 2.5 show the curvatures of the PI_V search space for one and two UPFC placements.

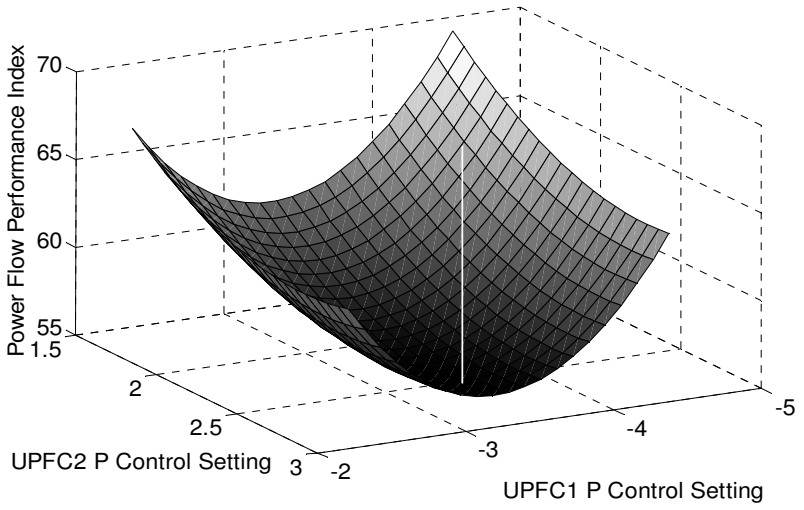

Figure. 2.3 *P* control for the two UPFC placements 5-8, 26-30 and SLC 23-32

For a single UPFC placement, the optimal *Q* setting is 0.46 p.u. For two UPFC placements on 5-8 and 26-30, the optimal *Q* settings are 0.014 p.u and 0.46 p.u,

respectively. The minimum PI_V for single placement and double placements are 0.28 and 0.28, respectively.

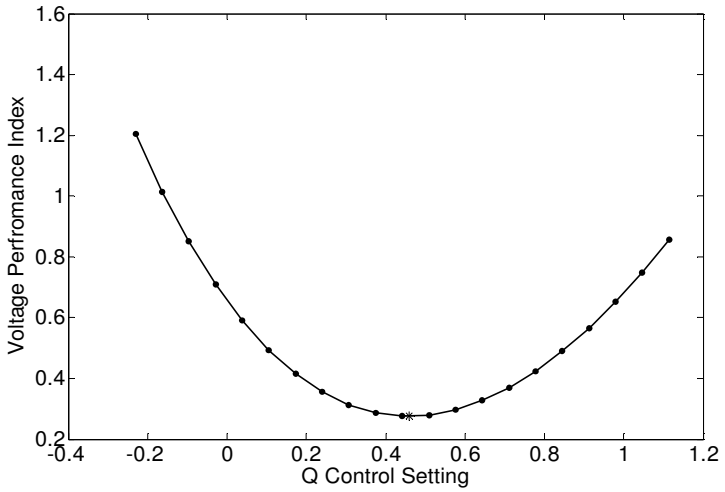

Figure. 2.4 *Q* control single UPFC placement 26-30 and SLC 23-32

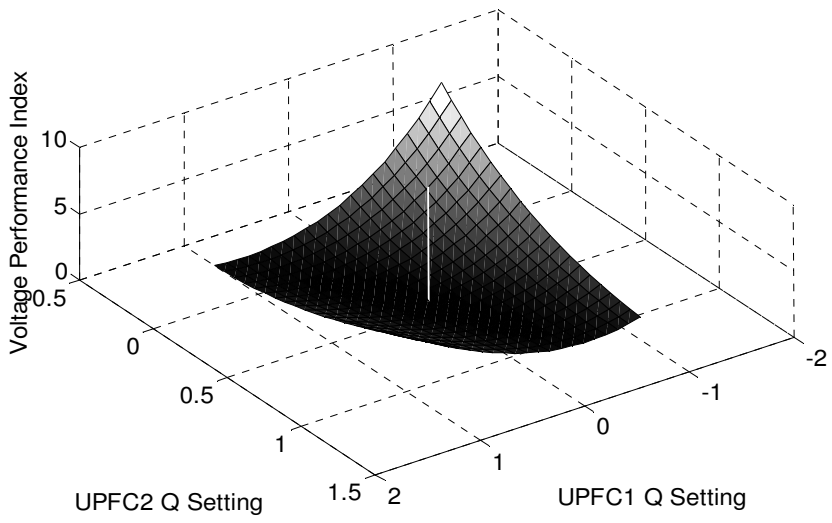

Figure. 2.5 *Q* control for the two UPFC placements 5-8, 26-30 and SLC 23-32

2.3 CONCLUSION

The numerical results for the *P* and *Q* control of one and two UPFCs are given in this section in the event of a SLC in the 118 bus system. As mentioned earlier, these support the theory of convexity and yield a single optimal setting based on their respective performance indices.

3. CONCLUSION

This dissertation proposed and implemented a fast, robust and reliable SQP based nonlinear optimization algorithm which successfully found the long term active and reactive power control settings of one or more UPFCs and mitigated overloads and voltage violations in various power systems. As the placement search space is very large, evolutionary algorithms are shown to be a good choice for the search of the near optimal placements. Further extension of this work may include implementation of the algorithm in real-time and interfacing it with dynamic control. Also, more analysis and insight into the search space for evolutionary algorithm application might help to find better placements through better initialization and pruning.

BIBLIOGRAPHY

1. V. Azbe, U. Gabrijel, D. Povh, and R. Mihalic, "The energy function of a general multimachine system with a Unified Power Flow Controller," *IEEE Transactions on Power Systems*, vol. 20, pp. 1478-1485, 2005.

2. S. N. Singh, K. S. Verma, and H. O. Gupta, "Optimal power flow control in open power market using Unified Power Flow Controller," *Power Engineering Society Summer meeting*, vol. 3, pp. 1698-1703, Jul 2001.

3. H. C. Leung and T. S. Chung, "Optimal power flow with a versatile FACTS controller by genetic algorithm," *IEEE Power Engineering Society Winter Meeting,* vol. 4, pp. 2806-2811, Jan 2000.

4. P. Bhasaputra and W. Ongsakul, "Optimal power flow with multi-type of FACTS devices by hybrid TS/SA approach," *IEEE International Conference on Industrial Technology*, vol. 1, pp. 285 – 290, Dec 2002.

5. T. Orfanogianni, and R. Bacher, "Steady-state optimization in power systems with series FACTS devices," *IEEE Transactions on Power Systems***,** vol 18, Issue 1, pp.19 – 26, Feb. 2003.

6. H. A. Abdelsalam, G. A. M. Aly, M. Abdelkrim and K. M. Shebl, "Optimal location of the Unified Power Flow Controller in electrical power systems," *IEEE PES Power Systems Conference and Exposition*, vol. 3, pp. 1391-1396, Oct 2004.

7. K. Visakha, D. Thukaram, L. Jenkins, H. P. Khincha, "Selection of UPFC suitable locations for system security improvement under normal and network contingencies*," Conference on Convergent for Asia-Pacific Region Technologies*, vol 2, pp. 755 – 760, 2003.

8. S. N. Singh and A. K. David, "A new approach for placement of FACTS devices in open power markets," *IEEE Power Engineering Review*, vol 21, pp. 58 – 60, 2001.

9. S. N. Singh and A. K. David, "Placement of FACTS devices in open power market," *International Conference on Advances in Power System Control, Operation and Management*, vol 1, pp. 173 - 177, 2001.

10. P. Bhasaputra, W. Ongsakul, "Optimal power flow with multi-type of FACTS devices by hybrid TS/SA approach," *IEEE International Conference on Industrial Technology*, vol 1, pp. 285 – 290, 2002.

11. A. Armbruster, M. Gosnell, B. McMillin and M. L. Crow, " The maximum flow algorithm applied to the placement and distributed steady-state control of UPFCs," *Proceedings of the 37th Annual North American Power Symposium,* pp. 77-83, 2005.

12. W. Shao and V. Vittal, "LP-based OPF for corrective FACTS control to relieve overloads and voltage viotlations," *IEEE Transactions on Power Systems*, vol. 21, No. 4, pp. 1832-1839, 2006.

VITA

Radha Padma Kalyani was born on August 15th 1978 in Andhra Pradesh, India. She received her Bachelors of Engineering from Andhra University, AP, India. She joined University of Missouri-Rolla in 2002 and received her Masters of Sciences in Electrical Engineering in 2003. She further continued her studies in the same department and received her PhD in Electrical Engineering in 2007. She has been an intern at Midwest ISO for two summer semesters. Her research interests include FACTS, power systems operation and control, optimization theory and energy markets.